(12) INTERNATIONAL APPLICATION PUBLISHED UNDER THE PATENT COOPERATION TREATY (PCT)

(19) World Intellectual Property Organization
International Bureau

(43) International Publication Date
12 September 2014 (12.09.2014)

WIPO | PCT

(10) International Publication Number
WO 2014/138529 A1

(51) International Patent Classification:
G01R 33/563 (2006.01) *A61B 5/055* (2006.01)

(21) International Application Number:
PCT/US2014/021546

(22) International Filing Date:
7 March 2014 (07.03.2014)

(25) Filing Language: English

(26) Publication Language: English

(30) Priority Data:
61/774,287 7 March 2013 (07.03.2013) US

(71) Applicant: **THE BOARD OF TRUSTEES OF THE UNIVERSITY OF ILLINOIS** [US/US]; 352 Henry Administration Bldg., 506 South Wright Street, Urbana, IL 61801 (US).

(72) Inventors: **MAGIN, Richard**; 4539 Franklin Ave, Western Springs, IL 60558 (US). **INGO, Carson**; 300 N State Street, Apt 5229, Chicago, IL 60654 (US).

(74) Agent: **GRABELSKY, David, A.**; McDonnell Boehnen Hulbert & Berghoff LLP, 300 South Wacker Drive, Chicago, IL 60606 (US).

(81) Designated States *(unless otherwise indicated, for every kind of national protection available)*: AE, AG, AL, AM, AO, AT, AU, AZ, BA, BB, BG, BH, BN, BR, BW, BY, BZ, CA, CH, CL, CN, CO, CR, CU, CZ, DE, DK, DM, DO, DZ, EC, EE, EG, ES, FI, GB, GD, GE, GH, GM, GT, HN, HR, HU, ID, IL, IN, IR, IS, JP, KE, KG, KN, KP, KR, KZ, LA, LC, LK, LR, LS, LT, LU, LY, MA, MD, ME, MG, MK, MN, MW, MX, MY, MZ, NA, NG, NI, NO, NZ, OM, PA, PE, PG, PH, PL, PT, QA, RO, RS, RU, RW, SA, SC, SD, SE, SG, SK, SL, SM, ST, SV, SY, TH, TJ, TM, TN, TR, TT, TZ, UA, UG, US, UZ, VC, VN, ZA, ZM, ZW.

(84) Designated States *(unless otherwise indicated, for every kind of regional protection available)*: ARIPO (BW, GH, GM, KE, LR, LS, MW, MZ, NA, RW, SD, SL, SZ, TZ, UG, ZM, ZW), Eurasian (AM, AZ, BY, KG, KZ, RU, TJ, TM), European (AL, AT, BE, BG, CH, CY, CZ, DE, DK, EE, ES, FI, FR, GB, GR, HR, HU, IE, IS, IT, LT, LU, LV, MC, MK, MT, NL, NO, PL, PT, RO, RS, SE, SI, SK, SM, TR), OAPI (BF, BJ, CF, CG, CI, CM, GA, GN, GQ, GW, KM, ML, MR, NE, SN, TD, TG).

Published:

— *with international search report (Art. 21(3))*

[Continued on next page]

(54) **Title**: FRACTIONAL ORDER AND ENTROPY BIO-MARKERS FOR BIOLOGICAL TISSUE IN DIFFUSION WEIGHTED MAGNETIC RESONANCE IMAGING

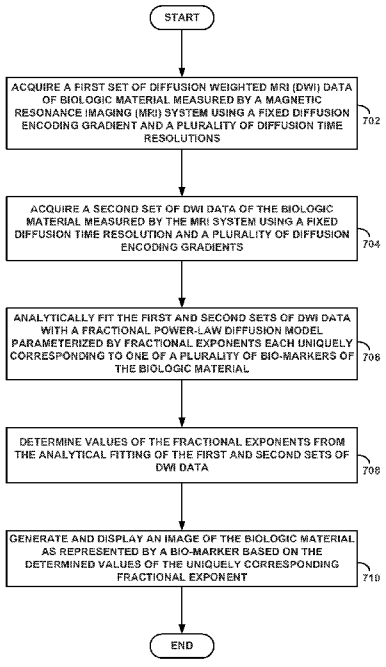


FIG. 7

(57) **Abstract**: The invention disclosed herein provides an example method and system for characterizing a biological structure in terms of bio-markers derived from DWI data. The methodology includes estimating bio-markers in a fixed diffusion time protocol, estimating bio-markers in fixed diffusion encoding gradient strength protocol, calculating parameters of a model, and using the parameters to characterize a biological structure. Using the techniques and methods described herein, the data may be used to identify structural degeneration, structural integrity and response to therapeutics.

WO 2014/138529 A1

— *before the expiration of the time limit for amending the claims and to be republished in the event of receipt of amendments (Rule 48.2(h))*

FRACTIONAL ORDER AND ENTROPY BIO-MARKERS FOR BIOLOGICAL TISSUE IN DIFFUSION WEIGHTED MAGNETIC RESONANCE IMAGING

BACKGROUND

Magnetic resonance imaging (MRI) is commonly used to image the internal tissues of a subject.

MRI is typically performed by placing the subject or object to be imaged at or near the isocenter of a strong, uniform magnetic field, B_0, known as the main magnetic field. The main magnetic field causes the atomic nuclei (spins) that possess a magnetic moment in the matter comprising the subject or object to become aligned in the magnetic field. The spins form a magnetization that precesses around the magnetic field direction at a rate proportional to the magnetic field strength. For hydrogen nuclei (which are the common nuclei employed in MRI), the precession frequency is approximately 64 MHz in a magnetic field of 1.5 Tesla. If the magnetization is perturbed by a small radio-frequency magnetic field, known as a B_1 magnetic field, the spins emit radiation at a characteristic radio frequency (RF). The emitted RF radiation can be detected and analyzed to yield information that may be used to produce an image of the subject or object. For purposes of the discussion herein, the term "object" will be used to refer to either a subject (e.g., a person) or an object (e.g., a test object) when describing magnetic resonance imaging of that "object."

In practice, magnetic field gradients are also applied to the subject or object in addition to the main magnetic field. The field gradients are typically applied along one or more orthogonal axes, (x, y, z), the z-axis usually being aligned with the B_0, and introduce spatially-distributed variations in frequency and/or phase of the precessing nuclear spins. By applying the radio-frequency B_1 magnetic field and gradient fields in carefully devised pulses and/or sequences of pulses that are switched on and off, the RF radiation emitted can carry spatially encoded information that, when detected and analyzed, can be used to produce detailed, high resolution images of the subject or object. Various techniques utilizing both specific pulse sequences and advanced image reconstruction methods have been developed, providing new advances, as well as introducing new challenges.

An MRI system typically includes hardware components, including a plurality of gradient coils positioned about a bore of a magnet, an RF transceiver system, and an RF switch controlled by a pulse module to transmit RF signals to and receive RF signals from an RF coil assembly. The received RF signals are also known as magnetic resonance (MR)

signal data. An MRI system also typically includes a computer programmed to cause the system to apply to an object in the system various RF signals, magnetic fields, and field gradients for inducing spin excitations and spatial encoding in an object, to acquire MR signal data from the object, to process the MR signal data, and to construct an MR image of the object from the processed MR signal data. The computer can include one or more general or special purpose processors, one or more forms of memory, and one or more hardware and/or software interfaces for interacting with and/or controling other hardward components of the MRI system.

MR signal data detected from an object are typically described in mathematical terms as "k-space" data (k-space is the 2D Fourier transform of the image). An image in actual space is produced by a Fourier transform of the k-space data. MR signal data are acquired by traversing k-space over the course of applying to the object the various RF pulses and magnetic field gradients. In practice, techniques for acquiring MR signal data from an object are closely related to techniques for applying the various RF pulses and magnetic field gradients to the object.

In diffusion weighted MRI (DWI) studies of neural tissue (e.g., human or other animal brain), a classical model assumes the statistical mechanics of Brownian motion and predicts a mono-exponential signal decay. However, some studies indicate signal decays which are not mono-exponential, particularly in the white matter. This deviation from the mono-exponential decay regime is called "anomalous diffusion." In neurodegenerative diseases, neural injuries, and neuroblastomas, the tissue microstructure in the brain is found to be altered from that of healthy neural tissue. In principle, DWI offers the non-invasive monitoring capability to measure microstructural changes via diffusion dynamics of water within the probed tissue to quantify the pathology.

In conventional DWI, a signal is modeled as the mono-exponential decay function, $\exp[-(bD)]$, where D is a classical diffusion coefficient and b is a MRI pulse sequence controlled parameter comprised of q (i.e., diffusion spatial resolution) and Δ (i.e., diffusion temporal resolution). To interpret the anomalous diffusion decay signal which is not mono-exponential, conventional techniques have been modified by applying: (1) a bi-exponential function, (e.g. $A\exp[-bD_1] + (1-A)\exp[-bD_2]$ where A is a volume fraction, D_1 is the fast diffusion coefficient, and D_2 is the slow diffusion coefficient); (2) a stretched exponential function (e.g., $\exp[-(bD)^w]$, where w is the stretching parameter over the entire b value; (3) a

stretched exponential function (e.g., $\exp[-(q^w \Delta D)]$, where w is the stretching parameter over the b-value component, q; and (4) a stretched exponential function (e.g., $\exp[-(q\Delta^w D)]$, where w is the stretching parameter over the b-value component, Δ.

Accordingly a need exists for a DWI protocol that is able to resolve diffusion patterns in neural tissue morphology, and for a comprehensive methodology for interpreting MRI anomalous diffusion decay signals.

SUMMARY

In spin-echo diffusion MRI experiments, signal decay is modeled with a mono-exponential as, $\exp(-bD)$ where b is the product of the q-space and diffusion time terms. As such, a diffusion-weighted experiment can be constructed with a set of b-values, with arbitrary weighting on the q and Δ components, so that a choice can be made to fix Δ and vary q in an array, or to fix q and vary Δ in an array.

A basic feature of Brownian motion is that the mean squared displacement (MSD) of diffusing particles grows linearly with time, $\langle x^2(t)\rangle \sim t$, provided three conditions are satisfied. Specifically: (1) increments are identically distributed with finite variance; (2) increments are independent (i.e., no "memory"); and (3) the process is continuous with an initial starting value set to zero. When any one of these conditions is not met, the diffusion process is called anomalous, and the MSD grows as a power law, $\langle x^2(t)\rangle \sim t^{\gamma}$. When $\gamma > 1$, the diffusion process is "super-diffusive," and when $0 < \gamma < 1$, the diffusion process is "sub-diffusive." For Brownian motion, the characteristic function can be represented by a mono-exponential decay process with respect to time. Likewise, in DWI, signal decay can also be modeled as mono-exponential decay, $\exp[-(bD)]$.

One practical approach to deriving the features of Brownian motion is the random walk (RW) model. In the RW model, the random walker's motion is governed by two stochastic processes: jump length distance and waiting time (between jump lengths). When these incremental processes are governed by a finite characteristic waiting time and jump length variance, in the continuum limit, the diffusion equation naturally arises (i.e., Fick's 2nd law). A generalization to the RW model can be obtained in the form of a continuous time random walk (CTRW) model, in which the incremental processes are no longer constrained by a Gaussian or Poissonian probability distribution function (pdf). Rather, the jump lengths and waiting times are governed by arbitrary and independent pdfs. In the most

general case, the random walker's motion is represented with fractional powers on the waiting time and jump length intervals, respectively. In this case, the MSD can be represented as a power law, $\langle x^2(t)\rangle \sim t^{2\alpha/\beta}$, where $0 < \alpha < 1$, and $0 < \beta < 2$. When $\alpha = 1$ and $\beta = 2$, the process returns to normal diffusion. When $2\alpha/\beta > 1$, the process becomes "super-diffusion." When $0 < 2\alpha/\beta < 1$, the process becomes "sub-diffusion." Solving the CTRW in the continuum limit yields a characteristic decay process that is represented by the Mittag-Leffler function (MLF), $E_\alpha(D_{\alpha,\beta}q^\beta\Delta^\alpha)$, where $D_{\alpha,\beta}$ is the diffusion coefficient with units space$^\beta$/time$^\alpha$. The MLF model is of interest because it relaxes *a priori* assumptions about the governing statistics of the diffusion process, and can identify normal, sub-, and super-diffusion regimes.

However, the MLF poses difficulties in practical implementation since the diffusion coefficient, $D_{\alpha,\beta}$, has fractional space and time units that are not necessarily directly measurable. Accordingly, to overcome this problem, example embodiments disclosed herein introduce a recast but equivalent form of the MLF model, expressed as $E_\alpha(D_{1,2}\tau^{1-\alpha}/\mu^{2-\beta}q^\beta\Delta^\alpha)$, in which $D_{1,2}$ is a diffusion coefficient having measurable units (e.g., mm^2/sec), made possible through parameters τ and μ. The coefficient $D_{1,2}$ is referred to herein as a "measurable diffusion coefficient."

More particularly, example embodiments herein provide two classes of DWI protocols (hereinafter "fixed Δ protocol" and "fixed q protocol") for operating an MRI system to obtain DWI data. Example embodiments herein further include techniques for fitting the recast MLF model to data obtained in DWI acquisitions according to the fixed Δ and fixed q protocols, in order to determine bio-markers derived from the recast MLF model.

Hence, in one aspect, various embodiments of the present invention provide a computer-implemented method for characterizing a biological structure, the method comprising: acquiring a first set of diffusion weighted MRI (DWI) data of biologic material, the first set of DWI data having been measured by a magnetic resonance imaging (MRI) system using a fixed diffusion encoding gradient and a plurality of diffusion time resolutions; acquiring a second set of DWI data of the biologic material, the second set of DWI data having been measured by the MRI system using a fixed diffusion time resolution and a plurality of diffusion encoding gradients; analytically fitting the first and second sets of DWI data with a fractional power-law diffusion model parameterized by fractional exponents each uniquely corresponding to one of a plurality of bio-markers of the biologic material;

determining values of the fractional exponents from the analytical fitting of the first and second sets of DWI data; and generating and displaying at least one image of the biologic material as represented by at least one of the plurality of bio-markers based on the determined values of the uniquely corresponding fractional exponent.

In another aspect, various embodiments of the present invention provide, in a magnetic resonance imaging (MRI) system, a method for characterizing a biological structure, the method comprising: acquiring a first set of diffusion weighted MRI (DWI) data of biologic material with the MRI system using a fixed diffusion encoding gradient and a plurality of diffusion time resolutions; acquiring a second set of DWI data of the biologic material with the MRI system using a fixed diffusion time resolution and a plurality of diffusion encoding gradients; analytically fitting the first and second sets of DWI data with a fractional power-law diffusion model parameterized by fractional exponents each uniquely corresponding to one of a plurality of bio-markers of the biologic material; determining values of the fractional exponents from the analytical fitting of the first and second sets of DWI data; and generating and displaying at least one image of the biologic material as represented by at least one of the plurality of bio-markers based on the determined values of the uniquely corresponding fractional exponent.

In a further aspect, various embodiments of the present invention provide a system comprising: one or more processors; memory; and machine-readable instructions stored in the memory that, when executed by the one or more processors, cause the system to carry out functions including: acquiring a first set of diffusion weighted MRI (DWI) data of biologic material, wherein the first set of DWI data comprise measurements made by a magnetic resonance imaging (MRI) system using a fixed diffusion encoding gradient and a plurality of diffusion time resolutions; acquiring a second set of DWI data of the biologic material, wherein the second set of DWI data comprise measurements made by the MRI system using a fixed diffusion time resolution and a plurality of diffusion encoding gradients; analytically fitting the first and second sets of DWI data with a fractional power-law diffusion model parameterized by fractional exponents each uniquely corresponding to one of a plurality of bio-markers of the biologic material; determining values of the fractional exponents from the analytical fitting of the first and second sets of DWI data; and generating and displaying at least one image of the biologic material as represented by at least one of the plurality of bio-markers based on the determined values of the uniquely corresponding fractional exponent.

In yet another aspect, various embodiments of the present invention a magnetic resonance imaging (MRI) system comprising: one or more processors; memory; a main magnet; one or more gradient coils; and machine-readable instructions stored in the memory that, when executed by the one or more processors, cause the MRI system to carry out functions including: acquiring a first set of diffusion weighted MRI (DWI) data of biologic material in the MRI system using a fixed diffusion encoding gradient and a plurality of diffusion time resolutions, acquiring a second set of DWI data of the biologic material in the MRI system using a fixed diffusion time resolution and a plurality of diffusion encoding gradients; analytically fitting the first and second sets of DWI data with a fractional power-law diffusion model parameterized by fractional exponents each uniquely corresponding to one of a plurality of bio-markers of the biologic material, determining values of the fractional exponents from the analytical fitting of the first and second sets of DWI data, and generating and displaying at least one image of the biologic material as represented by at least one of the plurality of bio-markers based on the determined values of the uniquely corresponding fractional exponent.

In accordance with example embodiments, the DWI bio-markers can be used to identify regimes of sub-, super-, and normal diffusion in neural tissue.

In further accordance with example embodiments, the DWI bio-markers can be used to distinguish healthy neural tissue from degenerated or injured neural tissue.

In accordance with example embodiments, the fixed Δ protocol can be used to identify anomalous diffusion in white matter and gray matter regions in healthy, degenerated, and injured neural tissue.

In accordance with example embodiments, the fixed q protocol can be used to identify anomalous diffusion, different from that identified in the fixed Δ protocol, in white matter and gray matter regions in healthy, degenerated, and injured neural tissue.

These as well as other aspects, advantages, and alternatives will become apparent to those of ordinary skill in the art by reading the following detailed description, with reference where appropriate to the accompanying drawings. Further, it should be understood that this summary and other descriptions and figures provided herein are intended to illustrate the invention by way of example only and, as such, that numerous variations are possible.

BRIEF DESCRIPTION OF THE DRAWINGS

Figure 1 is a flowchart illustrating a first estimation of model parameters, in accordance with example embodiments.

Figure 2 is a flowchart illustrating a second estimation of model parameters, in accordance with example embodiments.

Figure 3 illustrates a first example of DWI parameter maps of a rat brain, in accordance with example embodiments.

Figure 4 illustrates a second example of DWI parameter maps of a rat brain, in accordance with example embodiments.

Figure 5 illustrates a third example of DWI parameter maps of a rat brain, in accordance with example embodiments.

Figure 6 illustrates example DWI parameter maps of an epileptic rat brain, in accordance with example embodiments.

DETAILED DESCRIPTION

1. Overview

Example embodiments of the disclosed invention provide a methodology for characterizing a biological structure in terms of bio-markers derived from DWI data. The methodology includes estimating bio-markers in a fixed diffusion time protocol, estimating bio-markers in fixed diffusion encoding gradient strength protocol, calculating parameters of a model, and using the parameters to characterize a biological structure. Using the techniques and methods described herein, the data may be used to identify structural degeneration, structural integrity and response to therapeutics.

More particularly, example embodiments herein provide a "fixed Δ protocol" DWI protocol and a "fixed q protocol" DWI protocol for operating an MRI system to obtain DWI data. In example embodiments, a fixed Δ protocol can provide Δ fixed at a value in a range of $15 - 100$ ms, and a q value array set in a range of $0 - 200$ mm^{-1}, corresponding to gradient strengths of $0 - 1500$ mT / m. Example embodiments can further provide a fixed q protocol, in which q can be fixed at a value in a range of $15 - 100$ mm^{-1}, corresponding to gradient strengths of $100 - 1000$ mT / m, and a Δ value array can be set in a range of $15 - 250$ ms. Example embodiments herein further provide DWI bio-markers for neural

morphology, which are processed from the fixed Δ protocol and fixed q protocol DWI data. As described below, the bio-markers correspond to the parameters α, β, $D_{1,2}$, μ, τ of the recast MLF model introduced above, as well as an entropy H derived from the parameters. The techniques discussed herein can be adapted for application to other biologic material besides neural tissue.

To determine $D_{1,2}$, an "estimated measureable diffusion coefficient," D_m, is first obtained by fitting a mono-exponential function to the first three low b-value samples. After D_m has been obtained, two analogous stretched exponential fitting procedures are used to fit the fixed Δ protocol and fixed q protocol DWI data in order to find estimates of μ and τ, the estimated parameters denoted as $\bar{\mu}$ and $\bar{\tau}$ bar. The forms of the two analogous stretched exponential functions utilize the diffusion experiment pulse sequence parameters in order to independently constrain the magnitudes of $\bar{\mu}$ and $\bar{\tau}$ bar. Example flowcharts of the fitting procedures are shown in Figures 1 and 2. In order to fit the MLF, D_m, $\bar{\mu}$, $\bar{\tau}$, and $\alpha = 1$, $\beta = 2$ are used as starting values in order to converge upon values of $D_{1,2}$, μ, τ, α, and β.

As indicated in Figure 1, $\bar{\mu}$ and $\bar{\tau}$ are estimated using DWI data acquired according to the fixed Δ protocol. At step 102, the DWI data are fit with a stretched exponential expressed as $S/S_0 = \exp\left[-\left(bD_{\bar{\beta}}\right)^{\bar{\beta}}\right]$.

At step 104, an equivalency is set according to $\left(D_{\bar{\beta}}\right)^{\bar{\beta}} = D_m(\frac{\bar{\Delta}}{\bar{\mu}^2})^{1-\bar{\beta}}$.

At step 106, a solution for $\bar{\mu}$ is derived according to $\bar{\mu} = \sqrt{\bar{\Delta}}\left[\frac{\left(D_{\bar{\beta}}\right)^{\bar{\beta}}}{D_m}\right]^{\frac{1}{2(\beta-1)}}$.

At step 108, the DWI data are fit with an exponential $S/S_0 = \exp\left[-D_{\bar{\alpha}}\frac{1}{\bar{\mu}^2}(b\bar{\mu}^2)^{\bar{\alpha}}\right]$.

At step 110, an equivalency is set according to $D_{\bar{\alpha}} = D_m(\frac{\bar{\Delta}}{\bar{\tau}^{\bar{\alpha}}})$.

Finally, at step 112, a solution for $\bar{\tau}$ is derived according to $\bar{\tau} = \left(\bar{\Delta}\frac{D_m}{D_{\bar{\alpha}}}\right)^{\frac{1}{\bar{\alpha}}}$.

Figure 2 illustrates estimation of $\bar{\tau}$ and $\bar{\mu}$ using DWI data acquired according to the fixed q protocol. At step 202, the DWI data are fit with a stretched exponential expressed as $S/S_0 = \exp[-(bD_{\bar{\alpha}})^{\bar{\alpha}}]$.

At step 204, an equivalency is set according to $(D_{\bar{\alpha}})^{\bar{\alpha}} = D_m(q^2\bar{\tau})^{1-\bar{\alpha}}$.

At step 206, a solution for $\bar{\tau}$ is derived according to $\bar{\mu} = \frac{1}{q^2}\left[\frac{(D_{\bar{\alpha}})^{\bar{\alpha}}}{D_m}\right]^{\frac{1}{1-\alpha}}$.

At step 208, the DWI data are fit with an exponential $S/S_0 = \exp\left[-D_{\bar{\beta}}\bar{\tau}\left(\frac{b}{\bar{\tau}}\right)^{\bar{\beta}}\right]$.

At step 210, an equivalency is set according to $D_{\bar{\beta}} = D_m(\frac{\bar{\mu}^{\bar{\beta}}}{q^2})$.

Finally, at step 212, a solution for $\bar{\tau}$ is derived according to $\bar{\mu} = \left(q^2\frac{D_{\bar{\beta}}}{D_m}\right)^{\frac{1}{\bar{\beta}}}$.

In information theory, the amount of uncertainty in a stochastic process can be measured with Shannon information entropy (Shannon, "A mathematical theory of communication," Bell System Tech. Journal, 27:379-423, 1948). Considering information formulated in the context of statistical uncertainty can therefore provide tool to compare systems governed by differing stochastic processes, and their corresponding pdfs. For example, when comparing two alpha stable distributions, the Gaussian and the Cauchy, normalized with the same full-width, half maximum values, the Cauchy distribution can be shown to have greater information entropy. Non-Gaussian, or anomalous, diffusion phenomena have been correlated to regions of increased tissue complexity, such as white matter in the brain, which is relatively more anisotropic, heterogeneous, and tortuous compared to gray matter regions. From the information theory perspective, the white matter regions can thus be considered to have greater entropy than the gray matter regions, as they are governed by more uncertain diffusion pdfs.

Another approach to measure the uncertainty in a system is to analyze the characteristic function in terms of the Fourier transform in space with spectral entropy. Accordingly, example embodiments disclosed herein provide an entropy formalism for *b*-value diffusion decay signals as a function of q and Δ. The formalism derives from the MLF as a measure of the uncertainty of a characteristic function. As described below, after the MLF parameters are determined, a characteristic decay curve is reconstructed over the *b*-value range in either the fixed Δ protocol or fixed q protocol and the entropy in the diffusion process is computed as $H(q,\Delta)$.

Demonstration studies of the techniques provided in accordance with example embodiments disclosed herein were carried out using rat brains as test specimens of biologic material. More particularly, the fixed q and fixed Δ protocols were applied to acquisition of DWI data for a healthy rat brain and an epileptic rat brain. A brief summary of the results is presented below.

Application of the techniques provided in accordance with example embodiments is illustrated in Table 1, which shows that α separates the cerebral cortex, the central corpus callosum, and the striatum. In the fixed q protocol, α distinguishes the central corpus callosum from the lateral corpus callosum. In general, β shows less contrast than α and for the regions containing gray matter, $\beta \sim 2$, indicating Gaussian statistics on the jump length distributions. However, in the fixed Δ protocol, β separates the central corpus callosum from the regions containing gray matter. In the fixed Δ protocol, the measurable diffusion coefficient, $D_{1,2}$, separates the central corpus callosum from the striatum. In the fixed q protocol, μ separates the central corpus callosum from the regions containing gray matter. In the fixed Δ and fixed q protocols, τ separates the central corpus callosum from the regions containing gray matter. Numerical values for DWI MLF parameters in Table 1 are as follows: in the fixed Δ protocols, Δ_1 = 17.5 ms and Δ_2 = 50 ms, and fixed q protocols, $q_1 = 78$ mm^{-1} and $q_2 = 52$ mm^{-1}, on an axial slice through a healthy rat brain using a diffusion weighted stimulated echo pulse sequence.

Region of interest (ROI) analysis can be extended across the entire brain slice, which, by way of example, is represented as parameter maps in Figures 3-4. Specifically, Figure 3 illustrates DWI parameter maps for the fixed Δ protocol, $\Delta = 17.5$ ms, on an axial slice through a healthy rat brain using a diffusion-weighted stimulated echo pulse sequence. Figure 4 illustrates DWI parameter maps for the fixed q protocol, $q = 78$ mm^{-1}, on an axial slice through a healthy rat brain, on an axial slice through a healthy rat brain using a diffusion weighted stimulated echo pulse sequence.

Further application of the techniques is illustrated in Table 2, which shows that the entropy, $H(q,\Delta)$, in the MLF distinguishes the central corpus callosum from the lateral white matter. In the fixed Δ and q protocols, $H(q,\Delta)$ separates the cerebral cortex, the central corpus callosum, and the striatum. For comparison, the entropy, $H(q,\Delta)$ of the mono-exponential is shown in Table 2 to demonstrate the increased information provided in the MLF about the ROI. Numerical values for DWI entropy parameters in Table are as follows: in the fixed Δ protocols, Δ_1 = 17.5 ms and Δ_2 = 50 ms, and fixed q protocols, $q_1 = 78$ mm^{-1} and $q_2 = 52$ mm^{-1}, on an axial slice through a healthy rat brain using a diffusion weighted stimulated echo pulse sequence. The top row shows the contrast in the neural tissue produced

by the MLF. The bottom row shows the contrast in the neural tissue produced by the mono-exponential function

Further ROI analysis is extended across the entire brain slice, which is represented as parameter maps in Figure 5. More particularly, Figure 5 illustrates DWI entropy maps for the fixed Δ protocols, Δ_1 = 17.5 ms and Δ_2 = 50 ms, and fixed q protocols, q_1 = 78 mm^{-1} and q_2 = 52 mm^{-1}, on an axial slice through a healthy rat brain using a diffusion weighted stimulated echo pulse sequence. The left column shows the image contrast in the neural tissue produced by the MLF. The right column shows the image contrast in the neural tissue produced by the mono-exponential function.

Table 3 shows the ratio, $2\alpha/\beta$ as the composite exponent in the context of the trajectory of the MSD. In the fixed Δ protocol, all ROIs indicated sub-diffusion ($2\alpha/\beta < 1$), with the lateral corpus callosum regions growing slowest with respect to time. In the fixed Δ protocol, the corpus callosum ROIs are most sub-diffusive, whereas the cortex and striatum show slight sub-diffusion and effective normal diffusion ($2\alpha/\beta \sim 1$). In the fixed q protocol, the central corpus callosum ROI is most sub-diffusive, whereas the cortex and striatum show slight sub-diffusion and effective normal diffusion. Numerical values for DWI MLF parameter, $2\alpha/\beta$, in Table 3 are as follows: in the fixed Δ protocols, Δ_1 = 17.5 ms and Δ_2 = 50 ms, and fixed q protocols, q_1 = 78 mm^{-1} and q_2 = 52 mm^{-1}, on an axial slice through a healthy rat brain using a diffusion weighted stimulated echo pulse sequence.

Table 4 shows mean and standard deviation of the DWI MLF and entropy parameters for the fornix (F) ROIs in healthy and epileptic rat brains in the fixed Δ protocol, Δ = 17.5 ms.

Figure 6 shows a T2 weighted image of an age matched epileptic rat brain, with the lateral fornix ROIs circled in black. The fornix has been reported to significantly change in diffusion tensor imaging studies with a fractional anisotropy reduced by ~15% in epilepsy compared to healthy. Table 3 shows a comparison of fornix ROIs in healthy versus epileptic rat brains using the MLF and entropy parameters. There is a change in the MLF parameters, especially when considering the composite ratio in the power law growth of the mean-squared displacement, $2\alpha/\beta$ in which the healthy tissue is highly sub-diffusive ($2\alpha/\beta \sim 0.24 - 0.33$) and the degenerated tissue approaches Brownian motion ($2\alpha/\beta \sim 0.88 - 0.89$). Overall, this change is encoded with entropy, $H(q, \Delta)$, as a drastic loss

of information in the tissue structure going from healthy ($H(q, \Delta) \sim 0.90 - 0.91$) to epileptic ($H(q, \Delta) \sim 0.54 - 0.56$).

It should be noted that various changes and modifications to the presently preferred embodiments described herein will be apparent to those skilled in the art. Such changes and modifications may be made without departing from the spirit and scope of the present invention and without diminishing its attendant advantages.

2. Example Methods

Embodiments disclosed herein by way of example of fractional order and entropy bio-markers in DWI provide example techniques applicable in an MRI system or in a computer system at which DWI data can be accessed. As described above, an MRI system typically comprises hardware components including one or more gradient coils positioned about a bore of a magnet, an RF transceiver system, and an RF switch controlled by a pulse module to transmit RF signals to and receive RF signals from an RF coil assembly. The received RF signals are also known as magnetic resonance (MR) signal data. An MRI system also typically includes one or more computers programmed to cause the system to apply to an object in the system various RF signals, magnetic fields, and field gradients for inducing spin excitations and spatial encoding in an object, to acquire MR signal data from the object, to process the MR signal data, and to construct an MR image of the object from the processed MR signal data. The one or more computers can include one or more general or special purpose processors, one or more forms of memory, and one or more hardware and/or software interfaces for interacting with and/or controling other hardware components of the MRI system.

In example embodiments, fractional order and entropy bio-markers from DWI data can be determined by way of a computer-implemented method configured for execution by an MRI system or in a computer system at which DWI data can be accessed. The steps of the Figure 7 is a flowchart illustrating an example method in a computer system of determining fractional order and entropy bio-markers from DWI data.

At step **702**, a first set of diffusion weighted MRI (DWI) data of biologic material is acquired. The first set of DWI data corresponds to data measured by a magnetic resonance imaging (MRI) system using a fixed diffusion encoding gradient and a plurality of diffusion time resolutions.

At step **704**, a second set of DWI data of the biologic material is acquired. The second set of DWI data corresponds to measured by the MRI system using a fixed diffusion time resolution and a plurality of diffusion encoding gradients.

At step **706**, the first and second sets of DWI data are analytically fit with a fractional power-law diffusion model parameterized by fractional exponents that each uniquely corresponding to one of a plurality of bio-markers of the biologic material.

At step **708**, values of the fractional exponents are determined from the analytical fitting of the first and second sets of DWI data.

Finally, at step **710** at least one image of the biologic material is generated and displayed. In the image the biologic material is represented by at least one of the plurality of bio-markers based on the determine values of the uniquely corresponding fractional exponent. Figures 3-6 are examples of images representing a rat brain in one or another of the bio-markers described above.

In accordance with example embodiments, acquiring the first set of DWI data of the biologic material could entail acquiring the first set of DWI data from DWI data previously measured and provided for storage by the MRI system. Similarly, acquiring the second set of DWI data of the biologic material could entail acquiring the first set of DWI data from the DWI data previously measured and provided for storage by the MRI system. For example, the first and second sets of DWI data could be retrieved from an archive.

In accordance with example embodiments, the fixed diffusion encoding gradient and the plurality of diffusion time resolutions could correspond to DWI data measured using a diffusion spatial resolution with a value fixed in a range of 15 mm^{-1} — 100 mm^{-1}, and an array of diffusion temporal resolution values in a range of 15 ms — 250 ms. The diffusion spatial resolution range could correspond to a range of gradient strengths of 100 mT/m — 1000 mT/m.

In accordance with example embodiments, the fixed diffusion time resolution and the plurality of diffusion encoding gradients could correspond to DWI data measured using a diffusion temporal resolution with a value fixed in a range of 15 ms — 100 ms, and an array of diffusion spatial resolution values a range of 0 mm^{-1} — 200 mm^{-1}. The diffusion spatial resolution range could correspond to corresponding to a range of gradient strengths of 0 mT/m — 1500 mT/m.

In accordance with example embodiments, the fractional power-law diffusion model could include a mean square displacement (MSD) of a power-law form $\langle x^2(t)\rangle \sim t^{2\alpha/\beta}$, and has a solution expressed analytically as:

$$E_\alpha\left(\frac{D_{1,2}\tau^{1-\alpha}}{\mu^{2-\beta}} q^\beta \Delta^\alpha\right), \text{ in which}$$

α, β, μ, and τ are model parameters corresponding to four of the bio-markers,

$D_{1,2}$ is a measurable diffusion coefficient corresponding to a fifth bio-marker,

E_α is a Mittag-Leffler function (MLF),

and q is the diffusion spatial resolution, and Δ is the diffusion temporal resolution.

As discussed in connection with Equation *(13)* below, a mono-exponential model of signal decay in DWI can be expressed analytically as:

$$\frac{S}{S_0} = \exp(-bD),$$

and a stretched exponential model of signal decay in DWI is expressed analytically as:

$$\frac{S}{S_0} = \exp[-(bD)^w].$$

In these expressions, S_0 corresponds to an initial signal and S corresponds to a decaying signal, $b = q^2(\Delta - \delta/3)$, where Δ is the separation between gradient pulses of duration δ, and D is a classical diffusion coefficient. In the stretched exponential, w is a stretching parameter.

With these definitions, analytically fitting the first and second sets of DWI data with the fractional power-law diffusion model could entail first determining an estimated measurable diffusion coefficient D_m by analytically fitting a subset of the first and second sets of DWI data with a mono-exponential model of signal decay, then determining estimated values of μ and τ, $\bar{\mu}$ and $\bar{\tau}$, respectively, by (i) analytically fitting the first set of DWI data with a stretched exponential model of signal decay and $w = \alpha$, and (ii) analytically fitting the second set of DWI data with a stretched exponential model of signal decay and $w = \beta$, and finally determining $D_{1,2}$, α, β, μ, and τ by iteratively fitting the first and second sets of DWI data with the fractional power-law diffusion model using D_m, $\bar{\mu}$, $\bar{\tau}$, $\alpha = 1$, and $\beta = 2$ as starting values. These operations are illustrated by way of example in Figures 1 and 2, a discussed above.

In further accordance with example embodiments, the power law $\langle x^2(t)\rangle \sim t^{2\alpha/\beta}$ MSD of the fractional power-law diffusion model could be derived from a random walk (RW) model characterized by stochastic processes for jump-length distance and time between

jumps. In general the stochastic processes can have independent probability density functions (pdfs). The example method could then further include determining an entropy $H(q, \Delta)$ as a measure of uncertainty in the pdfs, the entropy $H(q, \Delta)$ being a sixth bio-marker.

In accordance with example embodiments, the biologic material could be neural tissue, such as a human brain.

Figure 8 is a flowchart illustrating an example method in an MRI system of determining fractional order and entropy bio-markers from DWI data. As noted in the discussion of the method illustrated in Figure 7, acquisition of the first and second sets of DWI data at steps **702** and **704** could entail accessing archived DWI data. The example method illustrated in Figure 8 differs in that both DWI data acquisition and the subsequent data analysis operations (including generating and displaying the images) are carried out by the MRI system. DWI data acquisition by the MRI system is made explicit in steps **802** and **804** below. Other than these two steps, steps **806-810** are the same as step **706-710** in the example method of Figure 7.

At step **802**, a first set of diffusion weighted MRI (DWI) data of biologic material is acquired with an MRI system using a fixed diffusion encoding gradient and a plurality of diffusion time resolutions.

At step **804**, a second set of DWI data of the biologic material is acquired with the MRI system using a fixed diffusion time resolution and a plurality of diffusion encoding gradients.

At step **806**, the first and second sets of DWI data are analytically fit with a fractional power-law diffusion model parameterized by fractional exponents that each uniquely corresponding to one of a plurality of bio-markers of the biologic material.

At step **808**, values of the fractional exponents are determined from the analytical fitting of the first and second sets of DWI data.

Finally, at step **810** at least one image of the biologic material is generated and displayed. In the image the biologic material is represented by at least one of the plurality of bio-markers based on the determine values of the uniquely corresponding fractional exponent. Again, Figures 3-6 are examples of images representing a rat brain in one or another of the bio-markers described above.

It will be appreciated that the example method steps of the example embodiment of method of determining fractional order and entropy bio-markers from DWI data can be

embodied as executable instructions stored on a non-transitory computer-readable medium, such as magnetic disk, CD-ROM, or the like. It will also be appreciated that the method steps described above can be modified or rearranged, and that additional steps can be added, without changing the scope or spirit of example embodiments herein.

3. Example Analytical Description

Without being limited to any theory of the underlying basis for the invention one of ordinary skill will appreciate the following features of the DWI methods set forth herein.

As noted above, diffusion decay processes can deviate from the mono-exponential model. The random walk (RW) model is a practical approach to derive the features of Brownian motion. In the RW model, the random walker's motion is governed by two stochastic processes: jump length distance, Δx, and waiting time (between jump lengths), Δt. When these incremental processes are governed by a finite characteristic waiting time and jump length variance, in the continuum limit as $\Delta x \rightarrow 0$ and $\Delta t \rightarrow 0$, the diffusion equation naturally arises (i.e., Fick's 2nd). A generalization to the RW model is the continuous time random walk (CTRW) model in which the incremental processes are no longer constrained by a Gaussian or Poissonian probability distribution function (pdf). Rather, the jump lengths and waiting times are governed by arbitrary and independent pdfs. In the most general case, the random walker's motion is represented with fractional powers α and β on the waiting time and jump length intervals, respectively, such that the MSD can be represented as a power law,

$$\langle x^2(t)\rangle \sim t^{2\alpha/\beta}, \qquad (1)$$

where $0 < \alpha \leq 1$ and $0 < \beta \leq 2$. When $2\alpha/\beta = 1$, the process is normal diffusion. When $2\alpha/\beta > 1$, the process is "super-diffusion." When $0 < 2\alpha/\beta < 1$, the process is "sub-diffusion." Solving the CTRW in the continuum limit yields a characteristic decay process that is represented by the Mittag-Leffler function (MLF). The MLF model is attractive in that it does not make *a priori* assumptions about the governing statistics of the diffusion process.

From RWs to CTRWs

In the context of RW theory in which the jump length variances and characteristic waiting times are finite, the one-dimensional Brownian motion of a diffusing particle, $P(x,t)$, in homogeneous and isotropic geometries can be described according to the second order partial differential equation,

$$\frac{\partial P(x,t)}{\partial t} = D\frac{\partial^2 P(x,t)}{\partial |x|^2}, \qquad (2)$$

where D is the diffusion coefficient. The solution to Equation *(2)* follows as the familiar Gaussian form,

$$P(x,t) = \frac{1}{\sqrt{4\pi Dt}}\exp(-\frac{x^2}{4\pi D}). \quad (3)$$

However, in the context of CTRW theory in which the jump length variances and characteristic waiting times follow asymptotic power law distributions, the one dimensional anomalous motion of a diffusing particle, $P(x,t)$, in heterogeneous biological tissues characterized by tortuous and porous geometries, can be described with a fractional partial differential equation of the form,

$${}_0^C\mathcal{D}_t^\alpha(P(x,t)) = D_{\alpha,\beta}\frac{\partial^\beta P(x,t)}{\partial|x|^\beta}, \quad (4)$$

where ${}_0^C\mathcal{D}_t^\alpha$ is the α^{th} $(0 < \alpha \leq 1)$ fractional order time derivative in the Caputo form, $\partial^\beta/\partial|x|^\beta$ is the β^{th} $(0 < \beta \leq 2)$ fractional order space derivative in the Reisz form, and $D_{\alpha,\beta}$ is the effective diffusion coefficient (e.g. mm$^\beta$/s$^\alpha$). The closed form solution of Equation *(4)* can be given in the Fox's H function,

$$P(x,t) = \frac{1}{\beta|x|}H_{3,3}^{2,1}\left[\frac{-|x|}{D_{\alpha,\beta}^{\frac{1}{\beta}}t^{\frac{2}{\beta}}}\middle|\begin{matrix}(1,\frac{1}{\beta}) & (\alpha,\frac{\alpha}{\beta}) & (1,\frac{1}{2})\\ (1,1) & (1,\frac{1}{\beta}) & (1,\frac{1}{2})\end{matrix}\right]. \quad (5)$$

When $\alpha = 1$ and $\beta = 2$, Equation *(4)* collapses to the Gaussian form in Equation *(3)*. However, the solution to Equation *(4)* can be more succinctly written by performing a Fourier transform in space ($P(x,t) \rightarrow p(k,t)$) to obtain the characteristic function,

$$p(k,t) = E_\alpha(-D_{\alpha,\beta}|k|^\beta t^\alpha), \quad (6)$$

where E_α is the single-parameter Mittag-Leffler function. The MLF is a well-behaved function defined as a power series expansion,

$$f(z) = E_\alpha(z) = \sum_{k=1}^{\infty}\frac{(z)^k}{\Gamma(\alpha k+1)}, \quad (7)$$

where the Γ function is the generalized form of the factorial function, defined for real numbers. When $\alpha = 1$ and $\beta = 2$, Equation *(6)* collapses to an exponential function in the Gaussian form with respect to k,

$$p(k,t) = \exp(-D_{1,2}|k|^2 t). \quad (8)$$

When $\alpha = 1$ and $0 < \beta < 2$, Equation *(6)* returns a stretched exponential function with respect to k,

$$p(k,t) = \exp(-D_{1,\beta}|k|^\beta t). \quad (9)$$

When $0 < \alpha < 1$ and $\beta = 2$, Equation *(6)* returns a stretched Mittag-Leffler function with respect to t,

$$p(k,t) = E_\alpha(-D_{\alpha,2}|k|^2 t^\alpha). \quad (10)$$

In the most general case of the solution to the diffusion equation shown in Equation *(6)*, the effective diffusion coefficient, $D_{\alpha,\beta}$, has units of space$^\beta$/time$^\alpha$. In order to formulate Equation *(6)* such that the diffusion coefficient can be written as $D_{1,2}$ with units of space^2/time, parameters μ (space) and τ (time) may be inserted to give,

$$p(k,t) = E_\alpha(-D_{1,2}\frac{\tau^{1-\alpha}}{\mu^{2-\beta}}|k|^\beta t^\alpha), \quad (11)$$

such that,

$$D_{\alpha,\beta} = D_{1,2}\frac{\tau^{1-\alpha}}{\mu^{2-\beta}}. \quad (12)$$

As $\alpha \to 1$ and $\beta \to 2$, the term $(\tau^{1-\alpha}/\mu^{2-\beta}) \to 1$, and, that is to show Equation *(11)* returns the Gaussian form in Equation *(8)*. The parameters, μ and τ, are needed as an empirical solution to preserve the units for the diffusion coefficient, however, others have derived analogs to these parameters (i.e., Δx, Δt) in conservation of mass problems and heavy tailed limit convergence of fractal and fractional dynamics.

From CTRW to Diffusion-Weighted MRI

In spin-echo diffusion MRI experiments, the signal decay, S, is modeled with a mono-exponential as,

$$S/S_0 = \exp(-bD), \quad (13)$$

where b is the product of the q-space and diffusion time terms, $b = q^2(\Delta - \delta/3)$. For brevity, the term $\bar{\Delta} = (\Delta - \delta/3)$ may be defined. As such, a diffusion-weighted experiment can be constructed with a set of b-values, with arbitrary weighting on the q and $\bar{\Delta}$ components, so that a choice can be made to fix $\bar{\Delta}$ and vary q in an array, or to fix q and vary $\bar{\Delta}$ in an array.

A stretched exponential can be fit to data obtained in fixed Δ, varying q experiments with a μ exponent and in fixed q, varying Δ experiments with an α exponent as an approach to independently interrogate fractional space and fractional time diffusion features. Expanding upon this, the generalized solution to the diffusion equation from CTRW theory in Equations *(6)* and *(11)* for modeling anomalous diffusion in MRI can be recast as,

$$p(q,\bar{\Delta}) = E_\alpha(-D_{1,2}\frac{\tau^{1-\alpha}}{\mu^{2-\beta}}|q|^\beta\bar{\Delta}^\alpha), \quad (14)$$

where β absorbs the square of the q term to operate as $0 < \beta \leq 2$. An entropy measure can additionally be used as a method to compare and contrast diffusion processes.

From Diffusion-Weighted MRI to Entropy in b-space

In information theory, the amount of uncertainty in a discrete probability density function, $P(x)$ can be measured with,

$$H_x = -\sum_{i=1}^{N} P(x_i)\ln(P(x_i)), \quad (15)$$

where H_x is the Shannon information entropy. Consideration of information formulated in the context of statistical uncertainty provides a tool to compare systems governed by differing stochastic processes. For example, when comparing two α-stable distributions, the Gaussian and the Cauchy, normalized with the same full-width, half maximum values, the Cauchy distribution can be shown to have greater information entropy. Non-Gaussian, or anomalous, diffusion phenomena have been correlated to regions of increased tissue complexity, like the white matter in the brain, which is relatively more anisotropic, heterogeneous, and tortuous compared to gray matter regions. From the information theory perspective, the white matter regions can be considered to have greater entropy than the gray matter regions as they are governed by more uncertain diffusion pdfs.

Another approach to measure the uncertainty in a system is to analyze the characteristic function in terms of the Fourier transform in space ($P(x,t) \rightarrow p(k,t)$) with spectral entropy,

$$H_k = -\sum_{i=1}^{N}\frac{\hat{p}(k_i)\ln(\hat{p}(k_i))}{\ln(N)}, \quad (16)$$

where $\hat{p}(k_i) = p(k_i)p^*(k_i)$ reflects the individual wavenumber's contribution to a normalized power spectrum of the Fourier transform, $p(k)$, and the term, $\ln(N)$ (i.e., discrete uniform distribution of N samples), is a normalization factor applied so that the spectral entropy, H_k, is between 0 and 1.

Furthermore, as Equation *(16)* is generally defined to measure the uncertainty of a characteristic function, we can adapt this formalism for b-value diffusion decay signals as a function of q and $\bar{\Delta}$,

$$H(q,\bar{\Delta}) = -\sum_{i=1}^{N}\frac{\hat{p}(k_i,\bar{\Delta})\ln(\hat{p}(k_i,\bar{\Delta}))}{\ln(N)}. \quad (17)$$

By inserting the characteristic function in Equation *(14)* (or, any definition of the characteristic function) into Equation *(17)*, the entropy in the diffusion process can be measured.

4. Example Procedure

To evaluate the MLF parameters in Equation *(14)* and the entropy, $H(q,\bar{\Delta})$, defined in Equation *(17)* as potential biomarkers for biological tissue features, demonstration diffusion-weighted MRI measurements were carried out to investigate the effects of arraying q vs. arraying Δ on one healthy fixed rat brain. The outcomes of this demonstration study can serve as a guide for the experimental setup of other studies, such as an inter-subject study on samples of healthy and epileptic fixed rat brains, as well as for diagnostic application of DWI. As the scope of this demonstration study was to investigate the effects of experimental setup on observed diffusion processes within the same biological tissue, one diffusion-weighted gradient direction was used. The y-axis diffusion weighting direction was chosen to evaluate the possibility of anomalous diffusion dynamics along the principal fiber direction of the corpus callosum. The effects of the diffusion weighting direction on the parameter values can be investigated in future studies to evaluate correlations to tensor metrics (e.g., first eigenvalue and fractional anisotropy).

Overnight, prior to imaging experiments, the rat brain was soaked in phosphate buffered saline. For the imaging experiment, the rat brain was placed in a 20 mm imaging tube, and the tube was filled with Fluorinert and secured with a magnetic susceptibility-matched plug to minimize vibrational movement due to the pulsed gradients. The rat brain was oriented in the spectrometer such that the anterior-posterior aligned with the main B0 field (z-axis), the superior-inferior with x-axis, and the lateral with the y-axis. At the Advanced Magnetic Resonance Imaging and Spectroscopy (AMRIS) Facility (Gainesville, Florida), pulsed gradient stimulated echo (PGSTE) diffusion-weighted experiments were performed on a Bruker spectrometer at 750 MHz (17.6 Tesla, 89 mm bore) with the following parameters: TR = 2 s, TE = 28 ms, b-values up to 25,000 s/mm^2, δ = 3.5 ms, NA = 2, y-axis diffusion weighting, 1 central slice in the y-z plane, slice thickness = 1 mm, FOV = 27x18 mm, matrix size of 142x94 pixels, in-plane resolution of 190 μm. It should be highlighted that in all experiments, $\delta \ll \Delta$ to ensure the short-pulse approximation remained valid. Variable TR data (TE = 12.5 ms, TR = 300−3600 ms, increments of 300 ms) were

collected to correct the PGSTE data for T1 relaxation effects. Additionally, the PGSTE data was Rician noise corrected.

Two constant Δ, variable q experiments were performed with Δ fixed at 17.5 and 50 ms. Two constant q, variable Δ experiments were performed with gradient strengths (g_y) at 350 and 525 mT/m to achieve q-values of 52 and 78 mm^{-1}, respectively. For the constant Δ=17.5 ms experiment, q was arrayed at 0, 39.7, 55.5, 67.7, 95.4, 116.7, 134.7, 150.5, 164.9, 178.1, and 190.3 mm^{-1}. For the constant Δ = 50 ms experiment, q was arrayed at 0, 24.9, 33.8, 40.9, 57.0, 69.4, 79.9, 89.2, 97.7, 105.4, 112.4 mm^{-1}. For the constant q =78 mm^{-1} experiment, Δ was arrayed at 17.5, 31.5, 45.5, 59.5, 73.5, 87.5, 101.5, 108.5, and 115 ms. For the constant q = 52 mm^{-1} experiment, Δ was arrayed at 17.5, 51.5, 85.5, 119.5, 153.5, 187.5, 221.5, 238.5, and 250 ms.

Because the generalized diffusion model in Equation *(14)* specifies $D_{1,2}$, μ, and τ as a ratio, any number of parameter value combinations can satisfy successful fitting results. To constrain these parameters, $D_{1,2}$, μ, and τ were first estimated using intermediate fits. To estimate the diffusion coefficient, a mono-exponential function was fit to the first 3 low b-value samples, referred to as, D_m above. After D_m estimation, two analogous stretched exponential fitting procedures were used to fit the constant $\bar{\Delta}$ and constant q experimental data in order to find estimates of $\bar{\tau}$ and $\bar{\mu}$ using, as discussed above in and illustrated in Figures 1 and 2.

Following the intermediate parameter estimations, D_m, $\bar{\tau}$, $\bar{\mu}$, α=1, β=2 were used as starting values in the non-linear least squared fit of the Mittag-Leffler function in order to converge upon $D_{1,2}$, μ, and τ, α, and β values. $D_{1,2}$, μ, and τ were allowed to float ±50% from their initial estimates. The value for α was bounded between 0 and 1.1 and β between 0 and 2.2.

After the MLF parameters were determined, the characteristic decay curve for $p(q, \bar{\Delta})$ was constructed using N=1,500 increments arrayed over variable q or variable $\bar{\Delta}$ for b-values between 0 and 25,000 s/mm^2. Then, the entropy (defined in Equation *(17)*) in the diffusion process, as modeled by the MLF, was computed as $H(q, \bar{\Delta})_{MLF}$. For comparison, using the mono-exponential model (D_m) in Equation *(13)*, a characteristic decay curve of N = 1,500 increments arrayed over b-values between 0 and 25,000 s/mm^2 was constructed. The entropy in the diffusion process, as modeled by the mono-exponential function, was computed as $H(q, \bar{\Delta})_{mono}$.

Results of the above procedure are discussed above in connection with Tables 1-4 and Figures 1-6.

An example embodiment of the present invention has been described above. Those skilled in the art will understand, however, that changes and modifications can be made to this embodiment without departing from the true scope and spirit of the invention, which is defined by the claims.

CLAIMS

What is claimed:

1. A computer-implemented method for characterizing a biological structure, the method comprising:

acquiring a first set of diffusion weighted MRI (DWI) data of biologic material, the first set of DWI data having been measured by a magnetic resonance imaging (MRI) system using a fixed diffusion encoding gradient and a plurality of diffusion time resolutions;

acquiring a second set of DWI data of the biologic material, the second set of DWI data having been measured by the MRI system using a fixed diffusion time resolution and a plurality of diffusion encoding gradients;

analytically fitting the first and second sets of DWI data with a fractional power-law diffusion model parameterized by fractional exponents each uniquely corresponding to one of a plurality of bio-markers of the biologic material;

determining values of the fractional exponents from the analytical fitting of the first and second sets of DWI data; and

generating and displaying at least one image of the biologic material as represented by at least one of the plurality of bio-markers based on the determined values of the uniquely corresponding fractional exponent.

2. The method of claim 1, wherein acquiring the first set of DWI data of the biologic material comprises acquiring the first set of DWI data from DWI data previously measured and provided for storage by the MRI system,

and wherein acquiring the second set of DWI data of the biologic material comprises acquiring the first set of DWI data from the DWI data previously measured and provided for storage by the MRI system.

3. The method of claim 1, wherein the fixed diffusion encoding gradient and the plurality of diffusion time resolutions comprises:

a diffusion spatial resolution with a value fixed in a range of 15 mm^{-1} — 100 mm^{-1}, and corresponding to a range of gradient strengths of 100 mT/m — 1000 mT/m; and

an array of diffusion temporal resolution values in a range of 15 ms — 250 ms.

4. The method of claim 1, wherein the fixed diffusion time resolution and the plurality of diffusion encoding gradients comprises:

a diffusion temporal resolution with a value fixed in a range of 15 ms — 100 ms; and

an array of diffusion spatial resolution values a range of 0 mm^{-1} — 200 mm^{-1}, and corresponding to a range of gradient strengths of 0 mT/m — 1500 mT/m.

5. The method of claim 1, wherein the fractional power-law diffusion model includes a mean square displacement (MSD) of a power-law form $\langle x^2(t)\rangle \sim t^{2\alpha/\beta}$, and has a solution expressed analytically as:

$$E_\alpha\left(\frac{D_{1,2}\tau^{1-\alpha}}{\mu^{2-\beta}}q^\beta\Delta^\alpha\right),$$

wherein α, β, μ, and τ are model parameters corresponding to four of the bio-markers,

wherein $D_{1,2}$ is a measurable diffusion coefficient corresponding to a fifth bio-marker,

wherein E_α is a Mittag-Leffler function (MLF),

wherein q is the diffusion spatial resolution, and Δ is the diffusion temporal resolution,

wherein a mono-exponential model of signal decay in DWI is expressed analytically as:

$$\frac{S}{S_0} = \exp(-bD),$$

wherein a stretched exponential model of signal decay in DWI is expressed analytically as:

$$\frac{S}{S_0} = \exp[-(bD)^w],$$

wherein S_0 is an initial signal and S is a decaying signal,

wherein $b = q^2(\Delta - \delta/3)$, and D is a classical diffusion coefficient,

wherein w is a stretching parameter,

and wherein analytically fitting the first and second sets of DWI data with the fractional power-law diffusion model comprises:

determining an estimated measurable diffusion coefficient D_m by analytically fitting a subset of the first and second sets of DWI data with a mono-exponential model of signal decay;

determining estimated values of μ and τ, $\bar{\mu}$ and $\bar{\tau}$, respectively, by (i) analytically fitting the first set of DWI data with a stretched exponential model of signal decay and $w = \alpha$, and (ii) analytically fitting the second set of DWI data with a stretched exponential model of signal decay and $w = \beta$; and

determining $D_{1,2}$, α, β, μ, and τ by iteratively fitting the first and second sets of DWI data with the fractional power-law diffusion model using D_m, $\bar{\mu}$, $\bar{\tau}$, $\alpha = 1$, and $\beta = 2$ as starting values.

6. The method of claim 5, wherein the power law $\langle x^2(t)\rangle \sim t^{2\alpha/\beta}$ MSD of the fractional power-law diffusion model derives from a random walk (RW) model having stochastic processes for jump-length distance and time between jumps, the stochastic processes having independent probability density functions (pdfs),

and wherein the method further comprises determining an entropy $H(q, \Delta)$ as a measure of uncertainty in the pdfs, the entropy $H(q, \Delta)$ being a sixth bio-marker.

7. The method of claim 1, wherein the biologic material comprises a human brain.

8. In a magnetic resonance imaging (MRI) system, a method for characterizing a biological structure, the method comprising:

acquiring a first set of diffusion weighted MRI (DWI) data of biologic material with the MRI system using a fixed diffusion encoding gradient and a plurality of diffusion time resolutions;

acquiring a second set of DWI data of the biologic material with the MRI system using a fixed diffusion time resolution and a plurality of diffusion encoding gradients;

analytically fitting the first and second sets of DWI data with a fractional power-law diffusion model parameterized by fractional exponents each uniquely corresponding to one of a plurality of bio-markers of the biologic material;

determining values of the fractional exponents from the analytical fitting of the first and second sets of DWI data; and

generating and displaying at least one image of the biologic material as represented by at least one of the plurality of bio-markers based on the determined values of the uniquely corresponding fractional exponent.

9. The method of claim 8, wherein the biologic material comprises a human brain.

10. A system comprising:

one or more processors;

memory; and

machine-readable instructions stored in the memory that, when executed by the one or more processors, cause the system to carry out functions including:

acquiring a first set of diffusion weighted MRI (DWI) data of biologic material, wherein the first set of DWI data comprise measurements made by a magnetic resonance imaging (MRI) system using a fixed diffusion encoding gradient and a plurality of diffusion time resolutions;

acquiring a second set of DWI data of the biologic material, wherein the second set of DWI data comprise measurements made by the MRI system using a fixed diffusion time resolution and a plurality of diffusion encoding gradients;

analytically fitting the first and second sets of DWI data with a fractional power-law diffusion model parameterized by fractional exponents each uniquely corresponding to one of a plurality of bio-markers of the biologic material;

determining values of the fractional exponents from the analytical fitting of the first and second sets of DWI data; and

generating and displaying at least one image of the biologic material as represented by at least one of the plurality of bio-markers based on the determined values of the uniquely corresponding fractional exponent.

11. The system of claim 10, wherein acquiring the first set of DWI data of the biologic material comprises acquiring the first set of DWI data from DWI data previously measured and provided for storage by the MRI system,

and wherein acquiring the second set of DWI data of the biologic material comprises acquiring the first set of DWI data from the DWI data previously measured and provided for storage by the MRI system.

12. The system of claim 10, wherein the fixed diffusion encoding gradient and the plurality of diffusion time resolutions comprises:

a diffusion spatial resolution with a value fixed in a range of 15 mm^{-1}—100 mm^{-1}, and corresponding to a range of gradient strengths of 100 mT/m —1000 mT/m; and

an array of diffusion temporal resolution values in a range of 15 ms — 250 ms.

13. The system of claim 10, wherein the fixed diffusion time resolution and the plurality of diffusion encoding gradients comprises:

a diffusion temporal resolution with a value fixed in a range of 15 ms 100 ms; and

an array of diffusion spatial resolution values a range of 0 mm^{-1} 200 mm^{-1}, and corresponding to a range of gradient strengths of 0 mT/m 1500 mT/m.

14. The system of claim 10, wherein the fractional power-law diffusion model includes a mean square displacement (MSD) of a power-law form $\langle x^2(t)\rangle \sim t^{2\alpha/\beta}$, and has a solution expressed analytically as:

$$E_\alpha\left(\frac{D_{1,2}\tau^{1-\alpha}}{\mu^{2-\beta}}q^\beta\Delta^\alpha\right),$$

wherein α, β, μ, and τ are model parameters corresponding to four of the bio-markers,

wherein $D_{1,2}$ is a measurable diffusion coefficient corresponding to a fifth bio-marker,

wherein E_α is a Mittag-Leffler function (MLF),

wherein q is the diffusion spatial resolution, and Δ is the diffusion temporal resolution,

wherein a mono-exponential model of signal decay in DWI is expressed analytically as:

$$\frac{S}{S_0} = \exp(-bD),$$

wherein a stretched exponential model of signal decay in DWI is expressed analytically as:

$$\frac{S}{S_0} = \exp[-(bD)^w],$$

wherein S_0 is an initial signal and S is a decaying signal,

wherein $b = q^2(\Delta - \delta/3)$, and D is a classical diffusion coefficient,

wherein w is a stretching parameter,

and wherein analytically fitting the first and second sets of DWI data with the fractional power-law diffusion model comprises:

determining an estimated measurable diffusion coefficient D_m by analytically fitting a subset of the first and second sets of DWI data with a mono-exponential model of signal decay;

determining estimated values of μ and τ, $\bar{\mu}$ and $\bar{\tau}$, respectively, by (i) analytically fitting the first set of DWI data with a stretched exponential model of signal decay and $w = \alpha$, and (ii) analytically fitting the second set of DWI data with a stretched exponential model of signal decay and $w = \beta$; and

determining $D_{1,2}$, α, β, μ, and τ by iteratively fitting the first and second sets of DWI data with the fractional power-law diffusion model using D_m, $\bar{\mu}$, $\bar{\tau}$, $\alpha = 1$, and $\beta = 2$ as starting values.

15. The system of claim 14, wherein the power law $\langle x^2(t)\rangle \sim t^{2\alpha/\beta}$ MSD of the fractional power-law diffusion model derives from a random walk (RW) model having stochastic processes for jump-length distance and time between jumps, the stochastic processes having independent probability density functions (pdfs),

and wherein the method further comprises determining an entropy $H(q, \Delta)$ as a measure of uncertainty in the pdfs, the entropy $H(q, \Delta)$ being a sixth bio-marker.

16. The system of claim 10, wherein the biologic material comprises a human brain.

17. A magnetic resonance imaging (MRI) system comprising:

one or more processors;

memory;

a main magnet;

one or more gradient coils; and

machine-readable instructions stored in the memory that, when executed by the one or more processors, cause the MRI system to carry out functions including:

acquiring a first set of diffusion weighted MRI (DWI) data of biologic material in the MRI system using a fixed diffusion encoding gradient and a plurality of diffusion time resolutions,

acquiring a second set of DWI data of the biologic material in the MRI system using a fixed diffusion time resolution and a plurality of diffusion encoding gradients;

analytically fitting the first and second sets of DWI data with a fractional power-law diffusion model parameterized by fractional exponents each uniquely corresponding to one of a plurality of bio-markers of the biologic material,

determining values of the fractional exponents from the analytical fitting of the first and second sets of DWI data, and

generating and displaying at least one image of the biologic material as represented by at least one of the plurality of bio-markers based on the determined values of the uniquely corresponding fractional exponent.

18. The MRI system of claim 17, wherein the biologic material comprises a human brain.

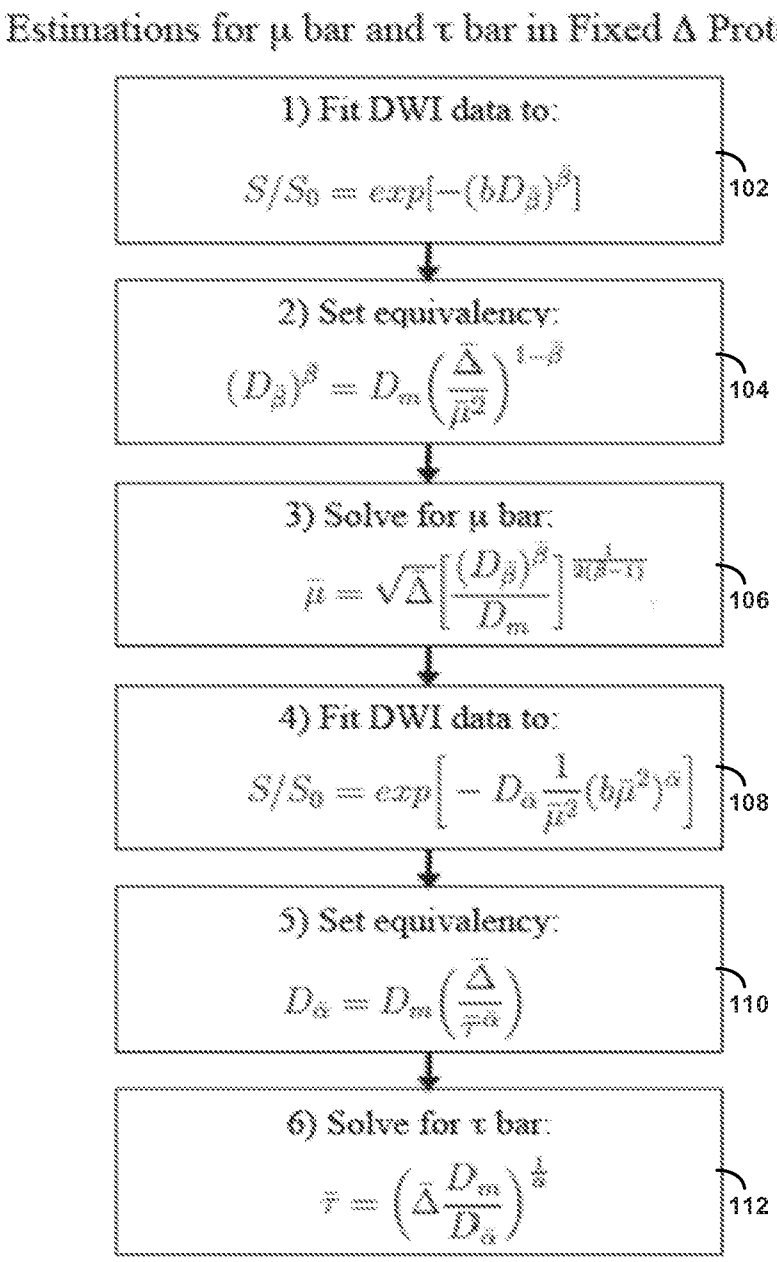

Estimations for μ bar and τ bar in Fixed Δ Protocol
1) Fit DWI data to:
$S/S_0 = exp[-(bD_\beta)^\beta]$
102
2) Set equivalency:
$(D_\beta)^\beta = D_m\left(\frac{\bar{\Delta}}{\bar{\mu}^2}\right)^{1-\beta}$
104
3) Solve for μ bar:
$\bar{\mu} = \sqrt{\bar{\Delta}}\left[\frac{(D_\beta)^\beta}{D_m}\right]^{\frac{1}{2\beta-1}}$
106
4) Fit DWI data to:
$S/S_0 = exp\left[-D_\alpha \frac{1}{\bar{\mu}^2}(b\bar{\mu}^2)^\alpha\right]$
108
5) Set equivalency:
$D_\alpha = D_m\left(\frac{\bar{\Delta}}{\bar{\tau}^2}\right)$
110
6) Solve for τ bar:
$\bar{\tau} = \left(\bar{\Delta}\frac{D_m}{D_\alpha}\right)^{\frac{1}{2\alpha}}$
112

FIG. 1

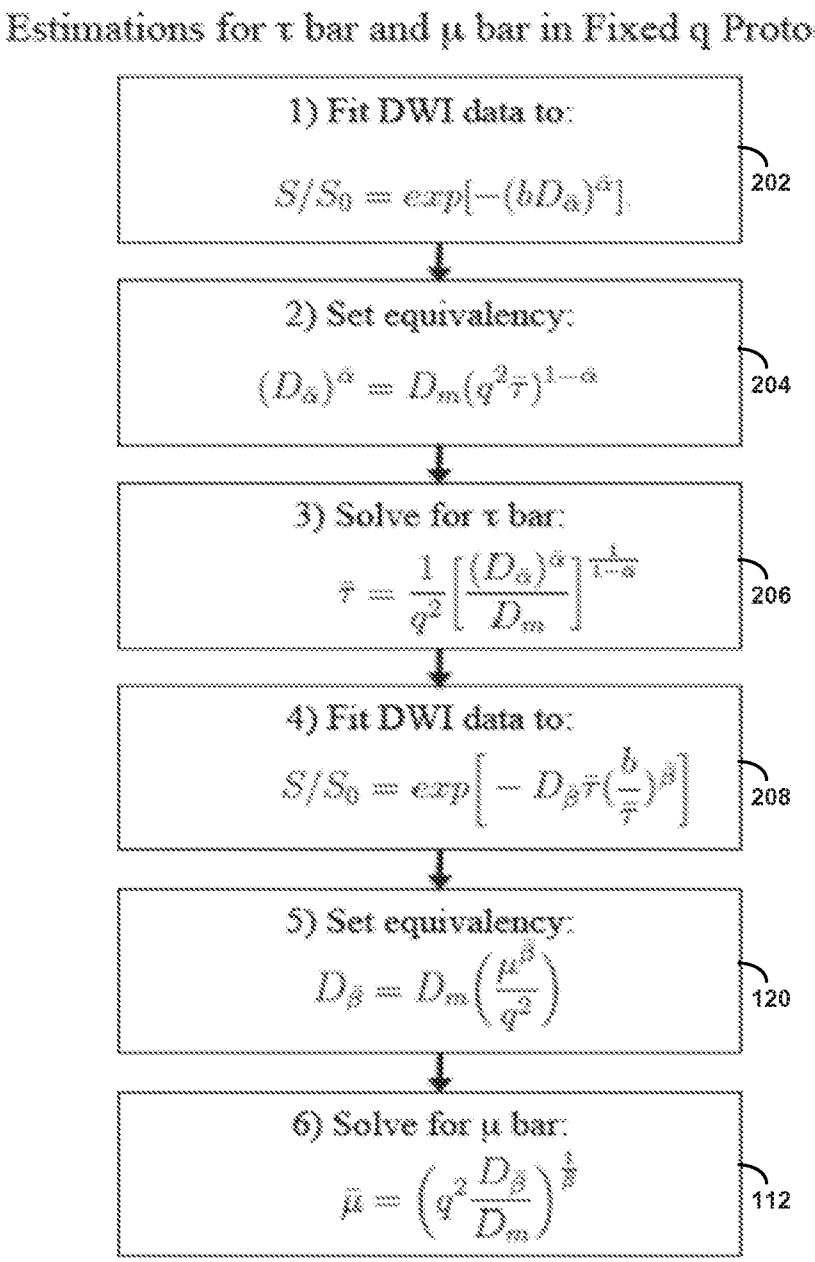

Estimations for τ bar and μ bar in Fixed q Protocol
1) Fit DWI data to:
$S/S_0 = exp[-(bD_a)^\alpha]$
202
2) Set equivalency:
$(D_a)^\alpha = D_m(q^2\bar{\tau})^{1-\alpha}$
204
3) Solve for τ bar:
$\bar{\tau} = \frac{1}{q^2}\left[\frac{(D_a)^\alpha}{D_m}\right]^{\frac{1}{1-\alpha}}$
206
4) Fit DWI data to:
$S/S_0 = exp\left[-D_\beta\bar{\tau}\left(\frac{b}{\bar{\tau}}\right)^\beta\right]$
208
5) Set equivalency:
$D_\beta = D_m\left(\frac{\bar{\mu}^\beta}{q^2}\right)$
120
6) Solve for μ bar:
$\bar{\mu} = \left(q^2\frac{D_\beta}{D_m}\right)^{\frac{1}{\beta}}$
112

FIG. 2

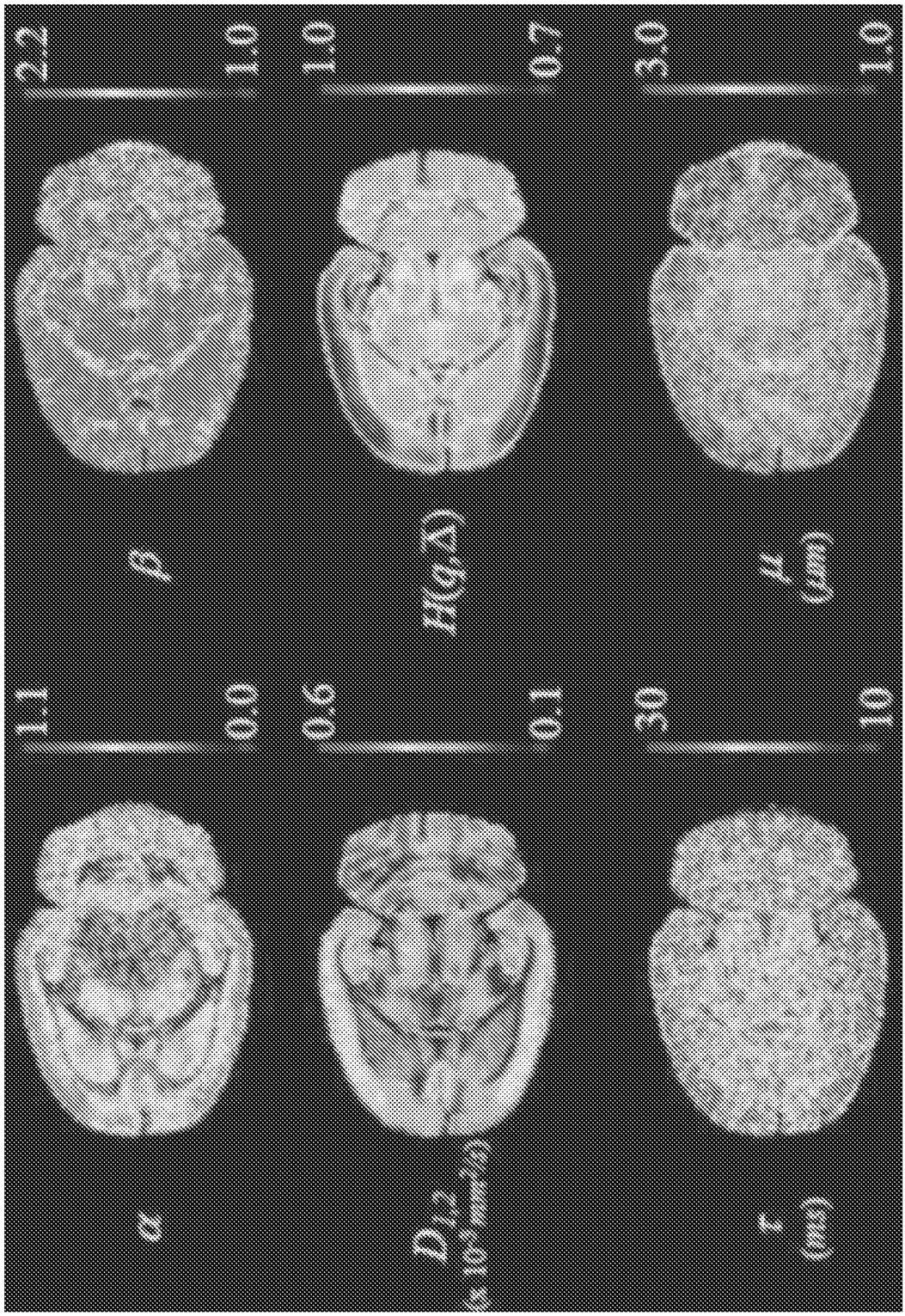


FIG. 3

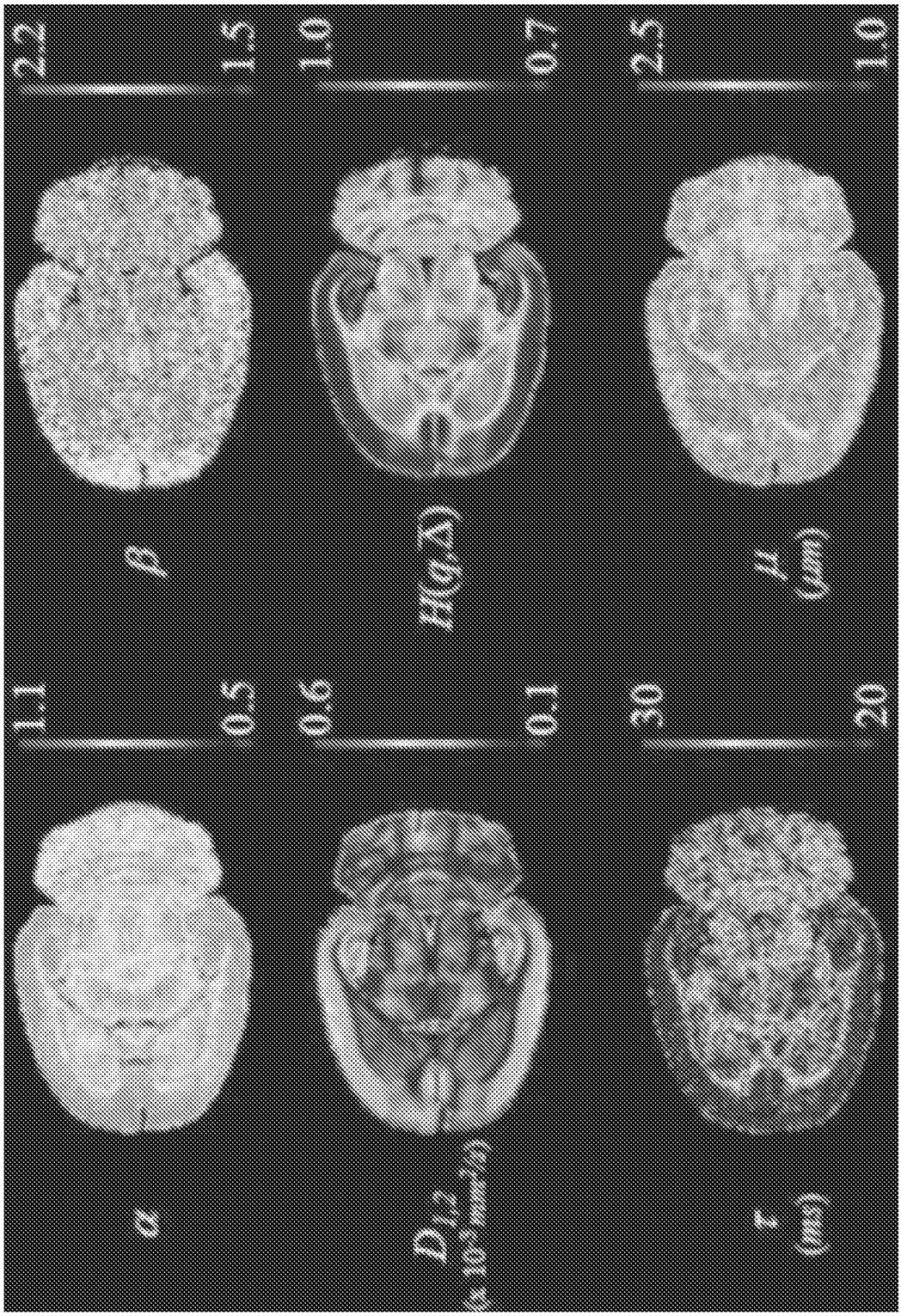


FIG. 4

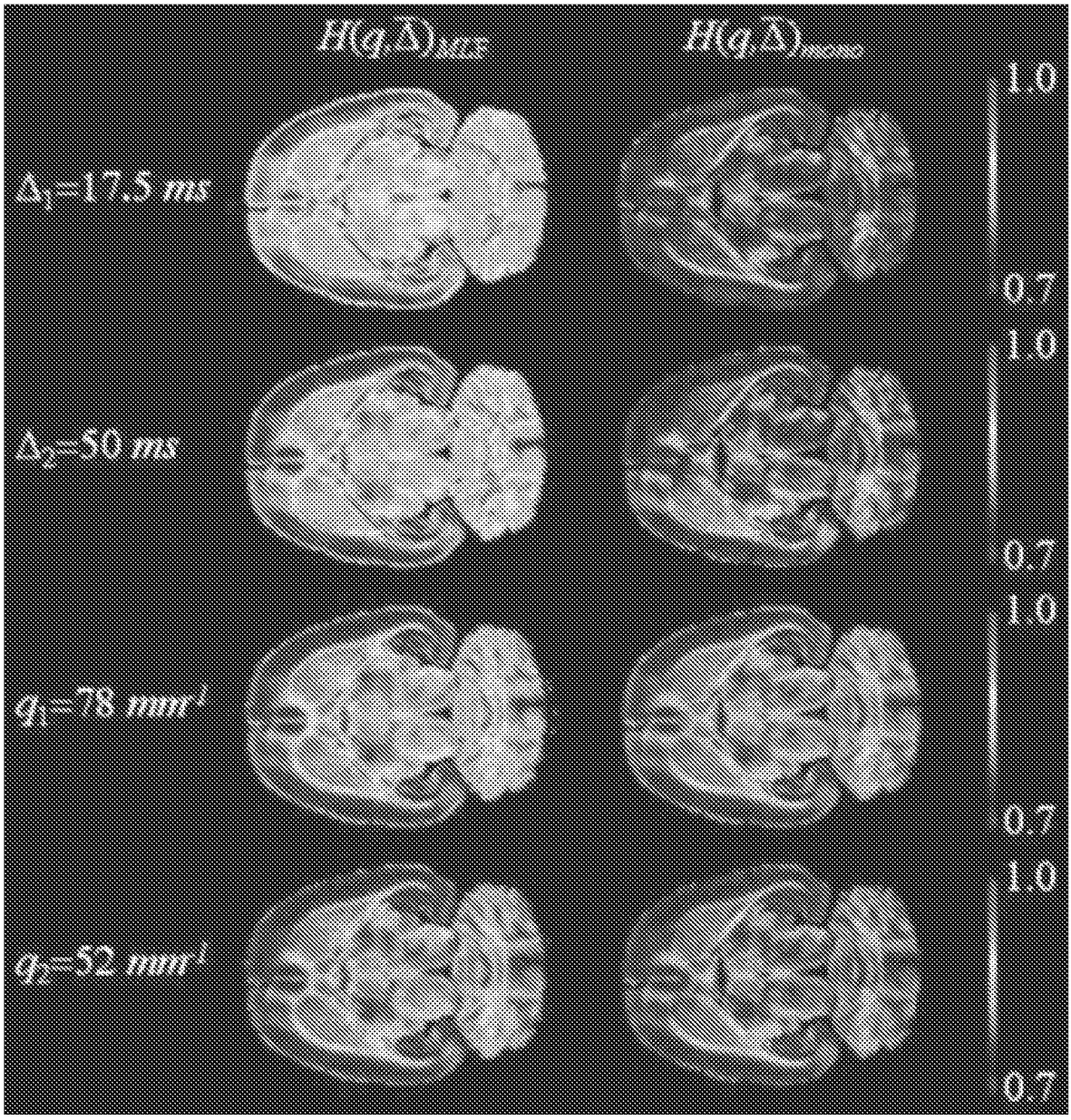

$H(q,\bar{\Delta})_{xyz}$
$H(q,\bar{\Delta})_{mean}$
Δ_1=17.5 ms
Δ_2=50 ms
q_1=78 mm^{-1}
q_2=52 mm^{-1}
1.0
0.7
1.0
0.7
1.0
0.7
1.0
0.7

FIG. 5

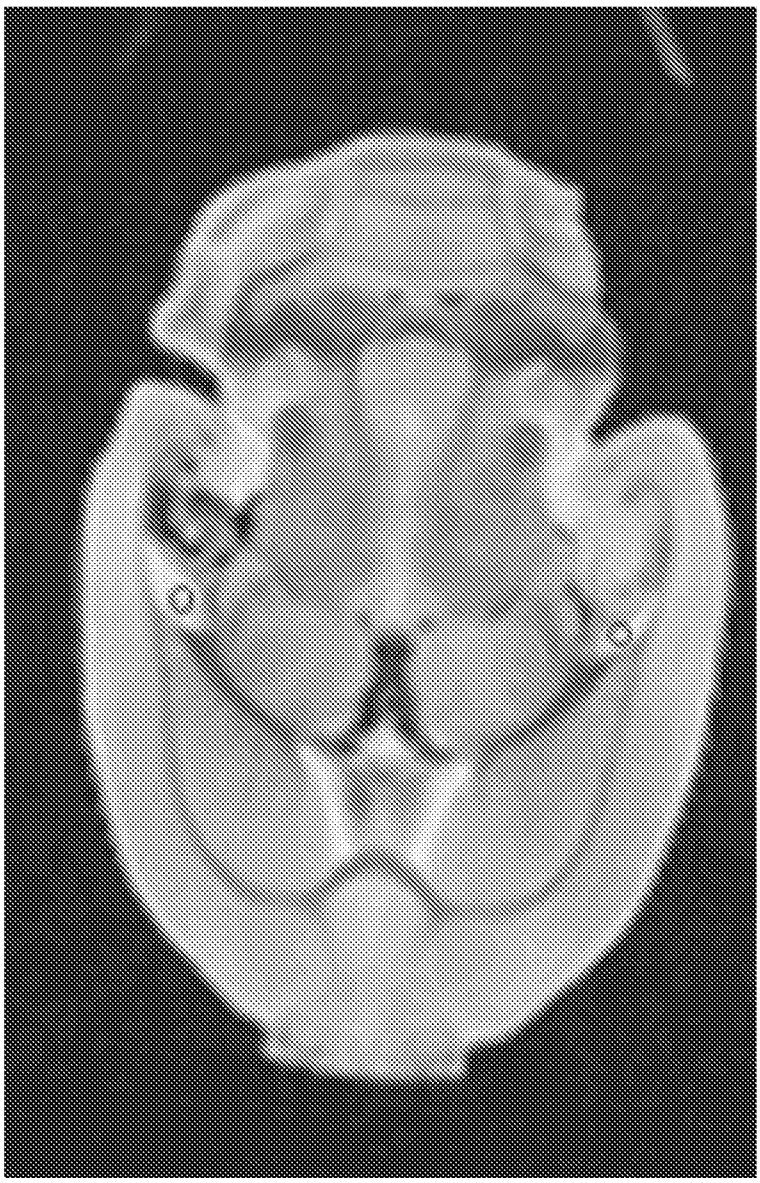


FIG. 6

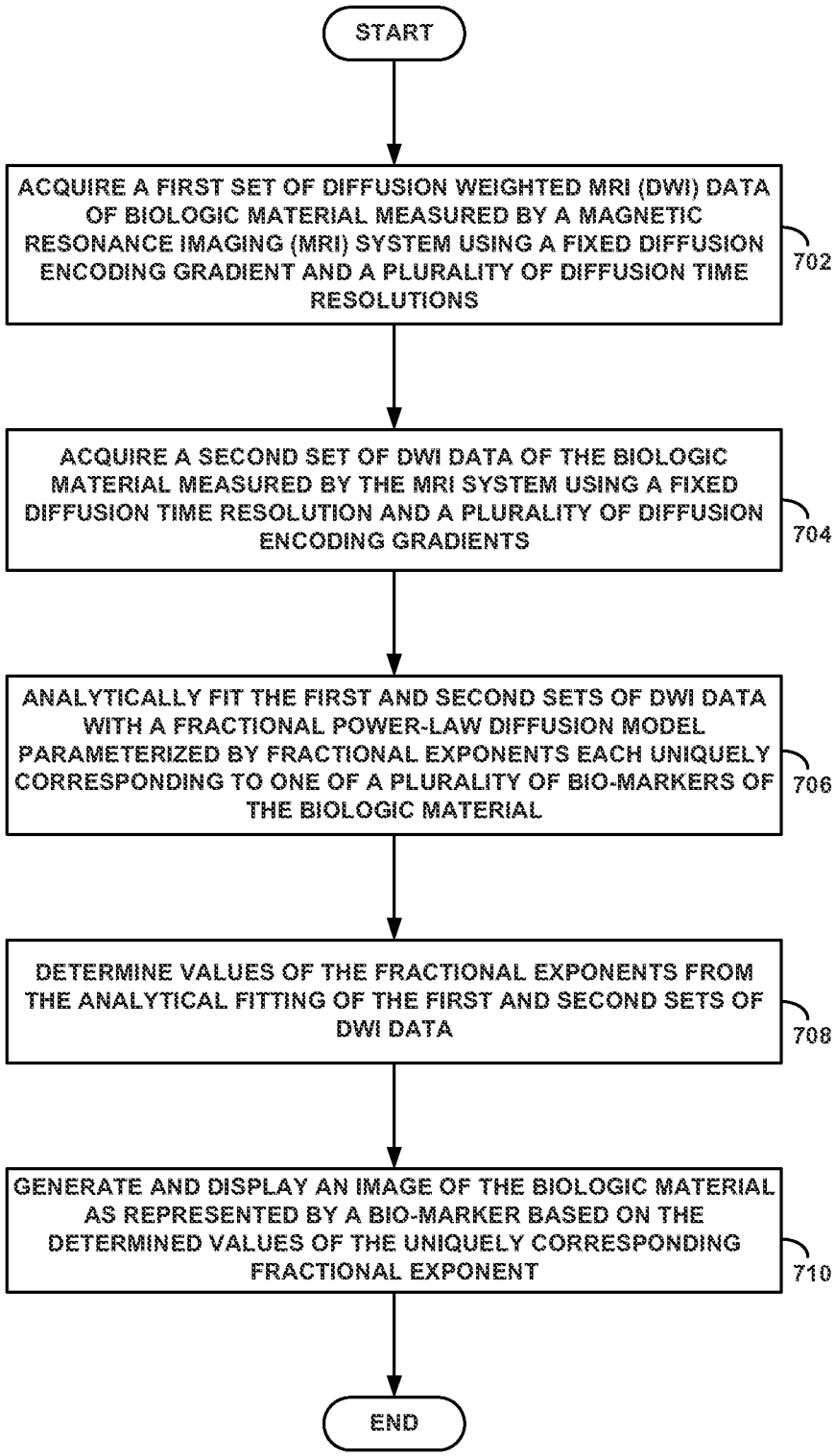

START
ACQUIRE A FIRST SET OF DIFFUSION WEIGHTED MRI (DWI) DATA OF BIOLOGIC MATERIAL MEASURED BY A MAGNETIC RESONANCE IMAGING (MRI) SYSTEM USING A FIXED DIFFUSION ENCODING GRADIENT AND A PLURALITY OF DIFFUSION TIME RESOLUTIONS
702
ACQUIRE A SECOND SET OF DWI DATA OF THE BIOLOGIC MATERIAL MEASURED BY THE MRI SYSTEM USING A FIXED DIFFUSION TIME RESOLUTION AND A PLURALITY OF DIFFUSION ENCODING GRADIENTS
704
ANALYTICALLY FIT THE FIRST AND SECOND SETS OF DWI DATA WITH A FRACTIONAL POWER-LAW DIFFUSION MODEL PARAMETERIZED BY FRACTIONAL EXPONENTS EACH UNIQUELY CORRESPONDING TO ONE OF A PLURALITY OF BIO-MARKERS OF THE BIOLOGIC MATERIAL
706
DETERMINE VALUES OF THE FRACTIONAL EXPONENTS FROM THE ANALYTICAL FITTING OF THE FIRST AND SECOND SETS OF DWI DATA
708
GENERATE AND DISPLAY AN IMAGE OF THE BIOLOGIC MATERIAL AS REPRESENTED BY A BIO-MARKER BASED ON THE DETERMINED VALUES OF THE UNIQUELY CORRESPONDING FRACTIONAL EXPONENT
710
END

FIG. 7

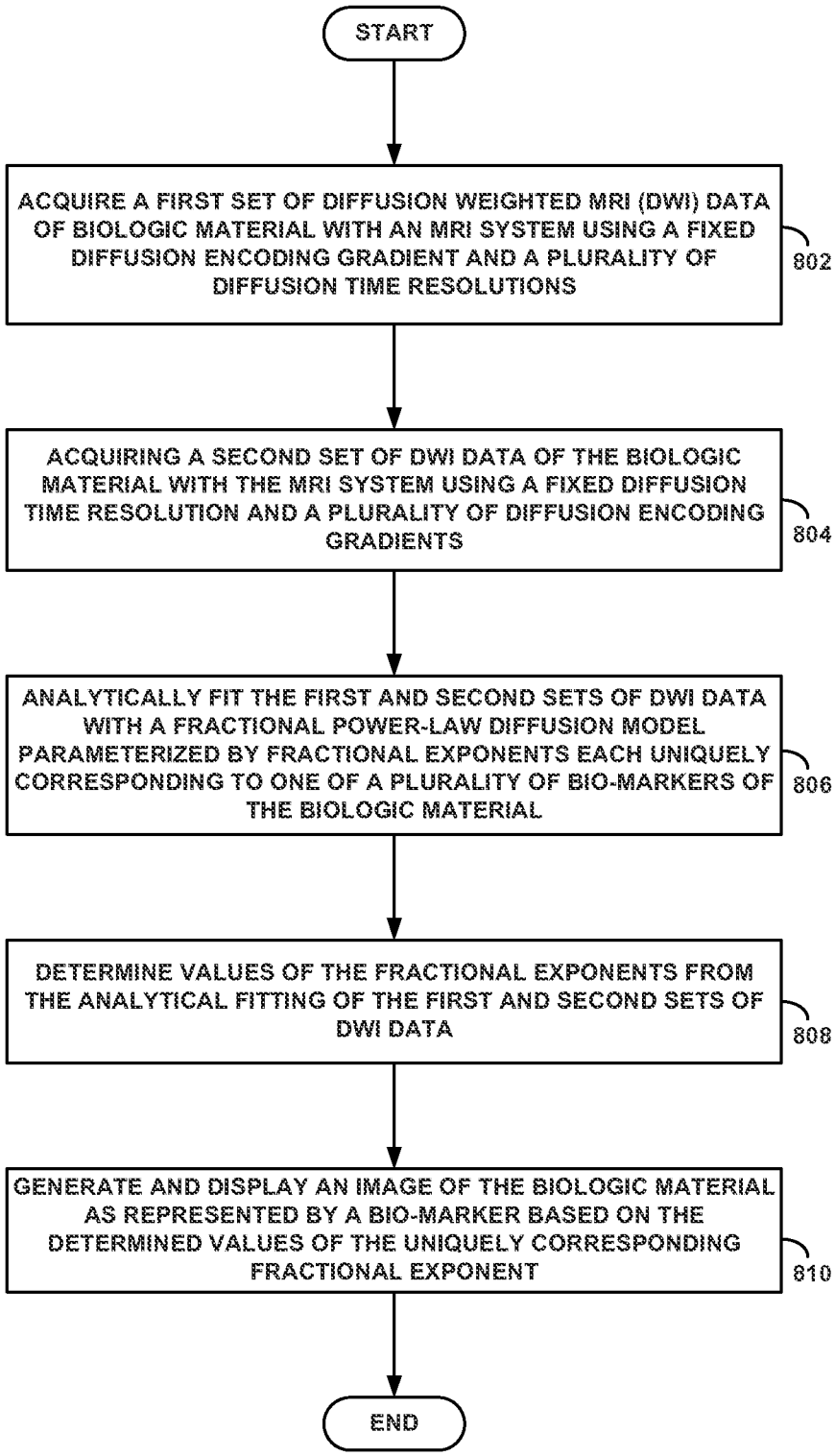

START
ACQUIRE A FIRST SET OF DIFFUSION WEIGHTED MRI (DWI) DATA OF BIOLOGIC MATERIAL WITH AN MRI SYSTEM USING A FIXED DIFFUSION ENCODING GRADIENT AND A PLURALITY OF DIFFUSION TIME RESOLUTIONS
802
ACQUIRING A SECOND SET OF DWI DATA OF THE BIOLOGIC MATERIAL WITH THE MRI SYSTEM USING A FIXED DIFFUSION TIME RESOLUTION AND A PLURALITY OF DIFFUSION ENCODING GRADIENTS
804
ANALYTICALLY FIT THE FIRST AND SECOND SETS OF DWI DATA WITH A FRACTIONAL POWER-LAW DIFFUSION MODEL PARAMETERIZED BY FRACTIONAL EXPONENTS EACH UNIQUELY CORRESPONDING TO ONE OF A PLURALITY OF BIO-MARKERS OF THE BIOLOGIC MATERIAL
806
DETERMINE VALUES OF THE FRACTIONAL EXPONENTS FROM THE ANALYTICAL FITTING OF THE FIRST AND SECOND SETS OF DWI DATA
808
GENERATE AND DISPLAY AN IMAGE OF THE BIOLOGIC MATERIAL AS REPRESENTED BY A BIO-MARKER BASED ON THE DETERMINED VALUES OF THE UNIQUELY CORRESPONDING FRACTIONAL EXPONENT
810
END

FIG. 8

MLF Parameter Values for ROIs In The Constant Δ_1 = 17.5 ms, Δ_2 = 50 ms, q_1 = 78 mm^{-1}, q_2 = 52 mm^{-1} Experiments (Y-Axis Diffusion Weighting)

parameter	ROI	Δ_1	Δ_2	q_1	q_2
α	(1) cortex, l	0.76 ± 0.05	0.92 ± 0.04	0.95 ± 0.01	0.96 ± 0.01
	(2) cortex, r	0.74 ± 0.06	0.92 ± 0.02	0.94 ± 0.01	0.95 ± 0.01
	(3) corpus callosum, l	0.40 ± 0.11	0.50 ± 0.25	0.82 ± 0.04	0.89 ± 0.02
	(4) corpus callosum, c	0.42 ± 0.04	0.39 ± 0.05	0.69 ± 0.05	0.80 ± 0.03
	(5) corpus callosum, r	0.33 ± 0.13	0.55 ± 0.18	0.82 ± 0.03	0.86 ± 0.04
	(6) striatum, l	0.58 ± 0.07	0.79 ± 0.09	0.89 ± 0.01	0.91 ± 0.02
	(7) striatum, r	0.57 ± 0.06	0.83 ± 0.03	0.91 ± 0.02	0.92 ± 0.01
β	(1) cortex, l	1.95 ± 0.06	1.76 ± 0.14	1.91 ± 0.03	1.98 ± 0.02
	(2) cortex, r	1.95 ± 0.08	1.99 ± 0.03	1.93 ± 0.04	1.90 ± 0.05
	(3) corpus callosum, l	1.79 ± 0.17	1.80 ± 0.16	1.91 ± 0.08	1.97 ± 0.04
	(4) corpus callosum, c	1.15 ± 0.13	1.42 ± 0.07	1.85 ± 0.07	1.96 ± 0.04
	(5) corpus callosum, r	1.82 ± 0.16	1.97 ± 0.09	1.88 ± 0.09	1.92 ± 0.05
	(6) striatum, l	1.99 ± 0.04	1.87 ± 0.14	1.98 ± 0.03	1.92 ± 0.03
	(7) striatum, r	2.00 ± 0.02	2.00 ± 0.04	1.98 ± 0.02	1.97 ± 0.03
$D_{1,2}$ ($\times 10^{-3} mm^2/s$)	(1) cortex, l	0.32 ± 0.01	0.35 ± 0.02	0.29 ± 0.01	0.32 ± 0.01
	(2) cortex, r	0.31 ± 0.01	0.26 ± 0.02	0.27 ± 0.01	0.28 ± 0.01
	(3) corpus callosum, l	0.32 ± 0.05	0.35 ± 0.11	0.26 ± 0.05	0.29 ± 0.05
	(4) corpus callosum, c	0.36 ± 0.04	0.35 ± 0.05	0.25 ± 0.02	0.30 ± 0.03
	(5) corpus callosum, r	0.34 ± 0.03	0.27 ± 0.03	0.26 ± 0.02	0.28 ± 0.02
	(6) striatum, l	0.27 ± 0.02	0.28 ± 0.01	0.24 ± 0.01	0.26 ± 0.01
	(7) striatum, r	0.28 ± 0.02	0.23 ± 0.01	0.24 ± 0.01	0.25 ± 0.01
μ (μm)	(1) cortex, l	2.39 ± 0.27	4.09 ± 0.22	2.15 ± 0.11	3.37 ± 0.54
	(2) cortex, r	2.40 ± 0.37	3.01 ± 0.97	2.12 ± 0.08	3.36 ± 0.29
	(3) corpus callosum, l	2.26 ± 0.27	3.94 ± 0.45	1.96 ± 0.13	3.38 ± 0.26
	(4) corpus callosum, c	2.44 ± 0.09	4.08 ± 0.36	1.82 ± 0.11	2.95 ± 0.17
	(5) corpus callosum, r	2.33 ± 0.06	3.29 ± 0.47	1.96 ± 0.05	3.23 ± 0.20
	(6) striatum, l	2.18 ± 0.29	3.86 ± 0.35	2.16 ± 0.10	3.45 ± 0.23
	(7) striatum, r	2.15 ± 0.35	2.97 ± 0.67	2.17 ± 0.11	3.49 ± 0.25
τ (ms)	(1) cortex, l	16.88 ± 1.48	50.62 ± 2.14	21.47 ± 1.17	30.98 ± 6.85
	(2) cortex, r	16.67 ± 1.65	54.46 ± 6.57	22.09 ± 1.89	33.88 ± 5.08
	(3) corpus callosum, l	19.94 ± 1.42	60.61 ± 6.71	25.50 ± 1.28	36.62 ± 6.99
	(4) corpus callosum, c	23.14 ± 1.41	67.50 ± 2.53	27.88 ± 2.05	41.21 ± 3.67
	(5) corpus callosum, r	20.25 ± 0.84	58.99 ± 2.89	25.57 ± 1.35	38.56 ± 3.97
	(6) striatum, l	18.39 ± 1.42	52.68 ± 3.17	23.80 ± 1.90	38.15 ± 7.80
	(7) striatum, r	18.78 ± 1.28	55.04 ± 2.78	22.87 ± 1.04	38.12 ± 4.21

Table 1

ENTROPY VALUES FOR THE ROIS IN THE CONSTANT $\Delta_1 = 17.5\,ms$, $\Delta_2 = 50\,ms$, $q_1 = 78\,mm^{-1}$, $q_2 = 52\,mm^{-1}$ EXPERIMENTS.

parameter	ROI	Δ_1	Δ_2	q_1	q_2
a. $H(q,\Delta)_{WM}$	(1) cortex, l	0.82 ± 0.01	0.78 ± 0.01	0.76 ± 0.01	0.76 ± 0.01
	(2) cortex, r	0.83 ± 0.01	0.81 ± 0.01	0.79 ± 0.01	0.78 ± 0.01
	(3) corpus callosum, l	0.88 ± 0.02	0.85 ± 0.03	0.83 ± 0.02	0.80 ± 0.02
	(4) corpus callosum, c	0.93 ± 0.01	0.91 ± 0.01	0.86 ± 0.02	0.83 ± 0.01
	(5) corpus callosum, r	0.88 ± 0.02	0.86 ± 0.03	0.83 ± 0.02	0.81 ± 0.02
	(6) striatum, l	0.86 ± 0.01	0.83 ± 0.01	0.82 ± 0.01	0.81 ± 0.01
	(7) striatum, r	0.86 ± 0.01	0.83 ± 0.01	0.82 ± 0.01	0.81 ± 0.01
b. $H(q,\Delta)_{GM}$	(1) cortex, l	0.76 ± 0.01	0.75 ± 0.01	0.78 ± 0.01	0.77 ± 0.01
	(2) cortex, r	0.77 ± 0.01	0.80 ± 0.01	0.79 ± 0.01	0.78 ± 0.01
	(3) corpus callosum, l	0.76 ± 0.02	0.76 ± 0.04	0.80 ± 0.02	0.78 ± 0.02
	(4) corpus callosum, c	0.74 ± 0.01	0.75 ± 0.02	0.81 ± 0.01	0.78 ± 0.01
	(5) corpus callosum, r	0.76 ± 0.01	0.79 ± 0.02	0.80 ± 0.01	0.78 ± 0.01
	(6) striatum, l	0.78 ± 0.01	0.79 ± 0.01	0.80 ± 0.01	0.79 ± 0.01
	(7) striatum, r	0.78 ± 0.01	0.81 ± 0.01	0.80 ± 0.01	0.80 ± 0.01

Table 2

$2\alpha/\beta$ COMPOSITE EXPONENT FOR THE ROIS IN THE CONSTANT $\Delta_1 = 17.5\,ms$, $\Delta_2 = 50\,ms$, $q_1 = 78\,mm^{-1}$, $q_2 = 52\,mm^{-1}$ EXPERIMENTS.

ROI	Δ_1	Δ_2	q_1	q_2
(1) cortex, l	0.76 ± 0.08	0.98 ± 0.09	0.98 ± 0.02	1.00 ± 0.03
(2) cortex, r	0.76 ± 0.08	0.92 ± 0.02	0.98 ± 0.03	0.99 ± 0.02
(3) corpus callosum, l	0.45 ± 0.12	0.57 ± 0.30	0.86 ± 0.04	0.91 ± 0.03
(4) corpus callosum, c	0.74 ± 0.12	0.54 ± 0.05	0.75 ± 0.05	0.84 ± 0.03
(5) corpus callosum, r	0.37 ± 0.16	0.56 ± 0.17	0.87 ± 0.05	0.87 ± 0.04
(6) striatum, l	0.62 ± 0.08	0.90 ± 0.13	0.90 ± 0.01	0.95 ± 0.03
(7) striatum, r	0.58 ± 0.06	0.83 ± 0.03	0.91 ± 0.02	0.94 ± 0.03

Table 3

parameter	ROI	Healthy	Epileptic
α	F, left	0.25 ± 0.10	0.86 ± 0.09
	F, right	0.35 ± 0.11	0.84 ± 0.07
β	F, left	1.64 ± 0.23	1.92 ± 0.12
	F, right	1.44 ± 0.22	1.88 ± 0.11
$2\alpha/\beta$	F, left	0.33 ± 0.12	0.89 ± 0.05
	F, right	0.24 ± 0.13	0.88 ± 0.03
$H(q,\Delta)$	F, left	0.90 ± 0.08	0.56 ± 0.04
	F, right	0.91 ± 0.06	0.54 ± 0.05

Table 4

INTERNATIONAL SEARCH REPORT

International application No
PCT/US2014/021546

A. CLASSIFICATION OF SUBJECT MATTER
INV. G01R33/563 A61B5/055
ADD.

According to International Patent Classification (IPC) or to both national classification and IPC

B. FIELDS SEARCHED

Minimum documentation searched (classification system followed by classification symbols)
G01R A61B

Documentation searched other than minimum documentation to the extent that such documents are included in the fields searched

Electronic data base consulted during the international search (name of data base and, where practicable, search terms used)
EPO-Internal, WPI Data

C. DOCUMENTS CONSIDERED TO BE RELEVANT

Category*	Citation of document, with indication, where appropriate, of the relevant passages	Relevant to claim No.
X	WO 2006/091983 A2 (UNIV FLORIDA [US]; OZARLSAN EVREN [US]; SHEPHERD TIMOTHY MICHAEL [US]) 31 August 2006 (2006-08-31) paragraph [0042] - paragraph [0069]; figure 8; table 1 -----	1-4, 7-13, 16-18
X	EVREN ÖZARSLAN ET AL: "Temporal scaling characteristics of diffusion as a new MRI contrast: Findings in rat hippocampus", NEUROIMAGE, vol. 60, no. 2, 26 January 2012 (2012-01-26), pages 1380-1393, XP055132889, ISSN: 1053-8119, DOI: 10.1016/j.neuroimage.2012.01.105 page 1381, column 1, paragraph 5 - page 1385, column 2, paragraph 1; figures 3,5 ----- -/--	1-4, 7-13, 16-18

[X] Further documents are listed in the continuation of Box C.

[X] See patent family annex.

* Special categories of cited documents :

"A" document defining the general state of the art which is not considered to be of particular relevance

"E" earlier application or patent but published on or after the international filing date

"L" document which may throw doubts on priority claim(s) or which is cited to establish the publication date of another citation or other special reason (as specified)

"O" document referring to an oral disclosure, use, exhibition or other means

"P" document published prior to the international filing date but later than the priority date claimed

"T" later document published after the international filing date or priority date and not in conflict with the application but cited to understand the principle or theory underlying the invention

"X" document of particular relevance; the claimed invention cannot be considered novel or cannot be considered to involve an inventive step when the document is taken alone

"Y" document of particular relevance; the claimed invention cannot be considered to involve an inventive step when the document is combined with one or more other such documents, such combination being obvious to a person skilled in the art

"&" document member of the same patent family

Date of the actual completion of the international search	Date of mailing of the international search report
6 August 2014	18/08/2014

Name and mailing address of the ISA/	Authorized officer
European Patent Office, P.B. 5818 Patentlaan 2 NL - 2280 HV Rijswijk Tel. (+31-70) 340-2040, Fax: (+31-70) 340-3016	Raguin, Guy

INTERNATIONAL SEARCH REPORT

International application No.
PCT/US2014/021546

Box No. II Observations where certain claims were found unsearchable (Continuation of item 2 of first sheet)

This international search report has not been established in respect of certain claims under Article 17(2)(a) for the following reasons:

1. ☐ Claims Nos.:
because they relate to subject matter not required to be searched by this Authority, namely:

2. ☒ Claims Nos.: 5, 6, 14, 15
because they relate to parts of the international application that do not comply with the prescribed requirements to such an extent that no meaningful international search can be carried out, specifically:
see FURTHER INFORMATION sheet PCT/ISA/210

3. ☐ Claims Nos.:
because they are dependent claims and are not drafted in accordance with the second and third sentences of Rule 6.4(a).

Box No. III Observations where unity of invention is lacking (Continuation of item 3 of first sheet)

This International Searching Authority found multiple inventions in this international application, as follows:

1. ☐ As all required additional search fees were timely paid by the applicant, this international search report covers all searchable claims.

2. ☐ As all searchable claims could be searched without effort justifying an additional fees, this Authority did not invite payment of additional fees.

3. ☐ As only some of the required additional search fees were timely paid by the applicant, this international search report covers only those claims for which fees were paid, specifically claims Nos.:

4. ☐ No required additional search fees were timely paid by the applicant. Consequently, this international search report is restricted to the invention first mentioned in the claims; it is covered by claims Nos.:

Remark on Protest

☐ The additional search fees were accompanied by the applicant's protest and, where applicable, the payment of a protest fee.

☐ The additional search fees were accompanied by the applicant's protest but the applicable protest fee was not paid within the time limit specified in the invitation.

☐ No protest accompanied the payment of additional search fees.

Continuation of Box II.2

Claims Nos.: 5, 6, 14, 15

The non-compliance with the substantive provisions of Art. 5 and 6 PCT (see below) is to such an extent that no meaningful assessment of novelty, an inventive step and industrial applicability of the subject-matter of claims 5, 6, 14 and 15 could be carried out at all (Art. 17(2) PCT).

1. Claims 5 and 14:

1.1 Not all of the variables used have been defined.

1.2 The terms "a mono-exponential model" and "a stretched exponential model" are defined twice. The second time, each term should be introduced with the definite article "the".

1.3 In view of the description (page 4, first two paragraphs) and the definition of claim 1 of "fractional exponents each uniquely corresponding to one of a plurality of bio-markers of the biologic material", there seems to be a contradiction with said definition and the model defined in claim 5 and in the description for the following reasons.

The fractional power-law diffusion model for the mean square displacement defined in claim 5 leads to the introduction of a diffusion coefficient with units of space^beta/time^alpha. The description and claim 5 then recast the problem by introducing three parameters, a "measurable diffusion coefficient" in its standard units along with a length scale and a time scale, to use parameters with common units. However, from a mathematical point-of-view, the problem does not change its nature and there should only be one independent parameter, such that the three parameters in the recast problem are not independent. It is understood that given the parameter estimation method defined in claim 5, maybe only one solution is obtained, but it may be an artifice from the numerical algorithm because mathematically one cannot simply change the dimensionality of a problem by replacing one parameter by two or more.

An analogous problem would be to recast the "measurable diffusion coefficient" as D_(1,2) = S / t, where S is a surface area and t is another time scale. It is obvious that a substance like e.g. water has an intrinsic self-diffusion coefficient D_H2O . After recasting the problem as above, water does not "magically" now have an intrinsic surface area and an intrinsic time scale. Indeed, for whatever time scale one would choose (or estimate), there would be a corresponding surface area S = D_H2O x t, i.e. there is still only one independent parameter.

Then, the wording

of claims 1 and 5 define that D_(1,2) ,tau and mu are different bio-markers of the biological material, which suggests that these three parameters are intrinsic properties of said biological material, while it cannot be true.

Therefore, there appears to be some misunderstanding or at least some missing information, such that there is alack of sufficient disclosure in that regard (Art. 5 PCT) and the subject-matter of claims 5 and 14 cannot be compared with the prior art.

2.
Claims 6 and 15 (which depend on claims 5 and 14, respectively):

The step of "determining an entropy" lacks clarity and support by the description in that it is unclear how said step is supposed to be carried out and the description only discloses one way to do so (see page 19-20), such that claims 6 and 15 should be limited accordingly.

The applicant's attention is drawn to the fact that claims relating to inventions in respect of which no international search report has been established need not be the subject of an international preliminary examination (Rule 66.1(e) PCT). The applicant is advised that the EPO policy when acting as an International Preliminary Examining Authority is normally not to carry out a preliminary examination on matter which has not been searched. This is the case irrespective of whether or not the claims are amended following receipt of the search report or during any Chapter II procedure. If the application proceeds into the regional phase before the EPO, the applicant is reminded that a search may be carried out during examination before the EPO (see EPO Guidelines C-IV, 7.2), should the problems which led to the Article 17(2) declaration be overcome.

INTERNATIONAL SEARCH REPORT

International application No
PCT/US2014/021546

C(Continuation). DOCUMENTS CONSIDERED TO BE RELEVANT

Category*	Citation of document, with indication, where appropriate, of the relevant passages	Relevant to claim No.
X	RICHARD L MAGIN ET AL: "Fractional order analysis of Sephadex gel structures: NMR measurements reflecting anomalous diffusion", COMMUNICATIONS IN NONLINEAR SCIENCE AND NUMERICAL SIMULATION, vol. 16, no. 12, 6 April 2011 (2011-04-06) , pages 4581-4587, XP028275453, ISSN: 1007-5704, DOI: 10.1016/J.CNSNS.2011.04.002 [retrieved on 2011-04-06] abstract page 4583, paragraph 1 - page 4584, paragraph 1	1-4, 7-13, 16-18
X,P	MAGIN RICHARD L ET AL: "Characterization of anomalous diffusion in porous biological tissues using fractional order derivatives and entropy", MICROPOROUS AND MESOPOROUS MATERIALS, vol. 178, 6 April 2013 (2013-04-06), pages 39-43, XP028595150, ISSN: 1387-1811, DOI: 10.1016/J.MICROMESO.2013.02.054 the whole document	1-4, 7-13, 16-18
X,P	CARSON INGO ET AL: "On random walks and entropy in diffusion-weighted magnetic resonance imaging studies of neural tissue", MAGNETIC RESONANCE IN MEDICINE, vol. 71, no. 2, 18 March 2013 (2013-03-18) , pages 617-627, XP055132799, ISSN: 0740-3194, DOI: 10.1002/mrm.24706 the whole document	1-4, 7-13, 16-18
T	RICHARD L MAGIN ET AL: "Spectral entropy in a fractional order model of anomalous diffusion", CARPATHIAN CONTROL CONFERENCE (ICCC), 2012 13TH INTERNATIONAL, IEEE, 28 May 2012 (2012-05-28), pages 458-463, XP032452457, DOI: 10.1109/CARPATHIANCC.2012.6228687 ISBN: 978-1-4577-1867-0 the whole document	

-/--

INTERNATIONAL SEARCH REPORT

International application No
PCT/US2014/021546

C(Continuation). DOCUMENTS CONSIDERED TO BE RELEVANT

Category*	Citation of document, with indication, where appropriate, of the relevant passages	Relevant to claim No.
T	MAGIN, RICHARD; INGO, CARSON: "ENTROPY AND INFORMATION IN A FRACTIONAL ORDER MODEL OF ANOMALOUS DIFFUSION", SYSTEM IDENTIFICATION - 16TH IFAC SYMPOSIUM ON SYSTEM IDENTIFICATION, 2012, vol. 16, no. 1, 11 August 2012 (2012-08-11), pages 428-433, XP009179492, DOI: 10.3182/20120711-3-BE-2027.00063 the whole document	
A	SUN H ET AL: "Variable-order fractional differential operators in anomalous diffusion modeling", PHYSICA A, NORTH-HOLLAND, AMSTERDAM, NL, vol. 388, no. 21, 1 November 2009 (2009-11-01), pages 4586-4592, XP026471217, ISSN: 0378-4371, DOI: 10.1016/J.PHYSA.2009.07.024 [retrieved on 2009-07-21] the whole document	1-4, 7-13, 16-18
A	HANYGA A ET AL: "Anisotropy in high-resolution diffusion-weighted MRI and anomalous diffusion", JOURNAL OF MAGNETIC RESONANCE, vol. 220, 14 May 2012 (2012-05-14), pages 85-93, XP028503730, ISSN: 1090-7807, DOI: 10.1016/J.JMR.2012.05.001 [retrieved on 2012-05-14] the whole document	1-4, 7-13, 16-18
A	PADHANI A R ET AL: "Diffusion-weighted magnetic resonance imaging as a cancer biomarker: Consensus and recommendations", NEOPLASIA, NEOPLASIA PRESS, ANN ARBOR, MI, US, vol. 11, no. 2, 1 February 2009 (2009-02-01), pages 102-125, XP007913484, ISSN: 1522-8002, DOI: 10.1593/NEO.81328 the whole document	1-4, 7-13, 16-18

-/--

INTERNATIONAL SEARCH REPORT

International application No
PCT/US2014/021546

C(Continuation). DOCUMENTS CONSIDERED TO BE RELEVANT

Category*	Citation of document, with indication, where appropriate, of the relevant passages	Relevant to claim No.
A	MAGIN ET AL: "Anomalous diffusion expressed through fractional order differential operators in the Bloch-Torrey equation", JOURNAL OF MAGNETIC RESONANCE, ACADEMIC PRESS, ORLANDO, FL, US, vol. 190, no. 2, 13 November 2007 (2007-11-13), pages 255-270, XP022427565, ISSN: 1090-7807, DOI: 10.1016/J.JMR.2007.11.007 the whole document	1-4, 7-13, 16-18
A	KÖPF M ET AL: "Anomalous Diffusion of Water in Biological Tissues", BIOPHYSICAL JOURNAL, CELL PRESS, US, vol. 70, 1 June 1996 (1996-06-01), pages 2950-2958, XP002385371, ISSN: 0006-3495 the whole document	1-4, 7-13, 16-18
A	KLEMM A ET AL: "Diffusion on random-site percolation clusters: theory and NMR microscopy experiments with model objects", PHYSICAL REVIEW E. STATISTICAL PHYSICS, PLASMAS, FLUIDS, AND RELATED INTERDISCIPLINARY TOPICS, AMERICAN INSTITUTE OF PHYSICS, NEW YORK, NY, US, vol. 65, no. 2 Pt 1, 1 February 2002 (2002-02-01), pages 21112-1, XP002385372, ISSN: 1063-651X, DOI: 10.1103/PHYSREVE.65.021112 the whole document	1-4, 7-13, 16-18
A	SHANNON C E: "THE MATHEMATICAL THEORY OF COMMUNICATION", MD COMPUTING, SPRINGER, NEW YORK, NY, US, vol. 14, no. 4, 1 January 1997 (1997-01-01), pages 306-317, XP000856516, ISSN: 0724-6811 cited in the application the whole document	1-4, 7-13, 16-18

INTERNATIONAL SEARCH REPORT

Information on patent family members

International application No
PCT/US2014/021546

Patent document cited in search report	Publication date	Patent family member(s)	Publication date
WO 2006091983 A2	31-08-2006	NONE	